Miniature Microscope for FRET Microscopy

Final Report

December 13, 2017

Team Members

John Rupel – Team Leader
Kaitlyn Gabardi – Communicator
Kadina Johnston – BWIG
Benjamin Ratliff -- BPAG
Ethan Nethery – BSAC

Client

Professor Matthew Merrins
Department of Medicine

Advisor

Professor Jeremy Rogers
Department of Biomedical Engineering

Table of Contents

1. Abstract

Microscopes are essential for understanding the structure of cells, microorganisms, and other molecular structures. Many educational institutions and scientists rely on these devices for important research, yet modern microscopes, while available to well-financed labs, are often not an option for a classroom. Therefore, students are unable to use these devices to practice processes they are expected to understand later. According to Nikon, typical epi-fluorescent microscope can cost over between $50,000 and $125,000, which exceeds a typical course budget. The client, Professor Matthew Merrins, teaches a human biochemistry lab at the University of Wisconsin-Madison. His lab currently uses Laconic, a Fluorescence Resonance Energy Transfer (FRET)-based biosensor [1] to detect the presence of Lactate in cells. Ideally, this class will allow students to learn about microscopy through experimentation, but with the cost constraint of the course, a modern microscope is out of the question. The goal of this design is to build an affordable, FRET-capable microscope that can be repeatedly manufactured for his students. The current proposed design involves a simplified microscope with a sample stand, a LED light source, an objective, a stage, a filter cube, filter-switching interface, a tube lens, and a camera. The images collected from the camera will be analyzed by software written by the team. The software will output quantitative results for students to analyze.

Commented [KJ1]: Add source

2. Introduction

2.1. Problem Statement

The client, Professor Matthew Merrins, teaches human biochemistry lab at the University of Wisconsin-Madison. The course focuses on the enzyme lactate dehydrogenase, which produces lactate from pyruvate. Currently, his lab utilizes Laconic, a Fluorescence Resonance Energy Transfer (FRET)-based biosensor. This biosensor detects the presence of lactate in healthy, living cells, but the fluorescence must be monitored over a period of time using an expensive microscope. This microscope excites the lactate biosensor using a complicated system of LEDs and filters. The fluorescence emission at two different wavelengths is recorded and a FRET efficiency ratio is calculated. Since the current microscope in his lab is expensive, the goal is to simplify the microscope and build a low-cost alternative specific to the Laconic biosensor. The client would like a working prototype by the end of the fall semester.

2.2. Project Motivation

Current microscopes are expensive due to their broad functionality. Even though this can be beneficial in a research lab, the client does not require as much flexibility for his simplified microscopes. The client would like to measure FRET, but with a specific focus on a single metabolic enzyme, lactate dehydrogenase. Ideally, he will have multiple devices for his class to maximize his students' educational experience. The design should be reproducible so that in the future he will have six to eight microscopes for his class.

2.3. Background

2.3.1 FRET

Fluorescence Resonance Energy Transfer (FRET) is the transfer of energy between two light-sensitive molecules. These molecules are known as chromophores, and they are referred to as the donor and the acceptor. FRET is a measurement of the different intensities of emission to determine the proximity of the two chromophores [1]. This is done by using a light source (usually an LED or laser) that will excite the donor chromophore. As the donor chromophore gets excited, it emits photons and transfers energy to excite the nearby acceptor chromophore; the transfer efficiency is a function of chromophore proximity. Usually the intensities of these sources are plotted on an absorption/emission spectrum, and a ratio of acceptor to donor emission intensity is obtained [2]. Many dynamic processes, such as protein-protein interactions, can be identified with various FRET biosensors. FRET is a popular method because of its ability to measure low concentration of molecules, and it has the capability to determine molecular dynamics of a given complex over time [3].

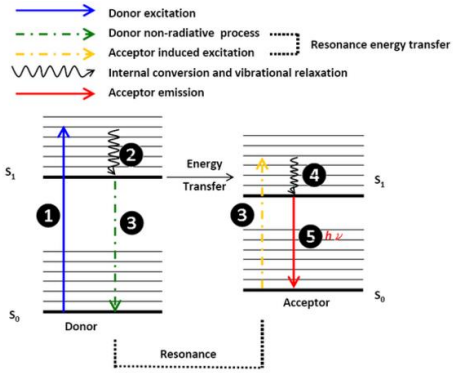

Figure 1. Schematic of Fluorescence Resonance Energy [2]. This image was obtained from the University of California, Davis, and shows of visual representation of FRET. S_0 represents the ground state, whereas S_f represents the lowest excited state after donor.

2.3.2 Laconic: Lactate Biosensor

Lactate is produced from pyruvate by the enzyme lactate dehydrogenase (LDH) in mammalian cells [1]. LDH is found in almost all body tissues, and it is vital in cellular respiration, signaling, and metabolic processes in healthy tissues [4]. In addition, if lactate is not regulated properly, this can lead to various risks to a person's health. Frequently, tumor cells have high rates of lactate production when oxygen is present [5]. As a result, many studies have been trying to further understand this process in living cells.

Professor Merrins' Lab specifically focuses on the nutrient metabolism in pancreatic islet beta cells. His goal is to further understand insulin release and how it can be regulated and tracked through low and high glucose conditions. By using rodents that are obese or have diabetes, Professor Merrins uses FRET to monitor metabolite production in different cells types, such as in yeast and cancer cells.

The biosensor that Professor Merrins hopes to use in his lab course is a protein that consists of two connected fluorophores and a lactate binding site [1]. This biosensor can be used to quantify lactate levels between 1 uM an 10 mM based on the FRET efficiency. Typical FRET sensors utilize cyan fluorescent protein (CFP) and yellow fluorescent protein (YFP), but these are not the only possible fluorophores [1]. Modifications have resulted in brighter and less pH-sensitive fluorophores, so the laconic biosensor, utilizes two of these: a monomeric teal fluorescent protein (mTFP) [6] and Venus [7], an improved YFP. Without lactate, the proteins are positioned well to allow for energy transfer between mTFP and Venus. With lactate, the proteins move such that there is much less energy transfer between them. The donor fluorophore is mTFP, which is excited by 430 nm light and fluoresces at 470 nm (Figure 2). The acceptor fluorophore is Venus, which is excited by light around 470 nm and fluoresces at 535 nm (Figure 3). Professor Merrins plans to run various experiments in his biochemistry class that will cause different behaviors of these fluorophores. One of his experiments involves subjecting the cells to high and low concentrations of glucose. High glucose concentration causes an increase in lactate production [8]. As lactate production increases, this causes the intensity of the mTFP channel to increase, and the intensity of the Venus channel to decrease. Therefore, the FRET ratio will decrease. When the cells are subjected to low concentration of glucose, mTFP decreases and

Venus increases which results in a larger FRET ratio. Professor Merrins' ideal device will be able to detect the difference in intensity between the two fluorophores, and overall determine the FRET ratio between experiments.

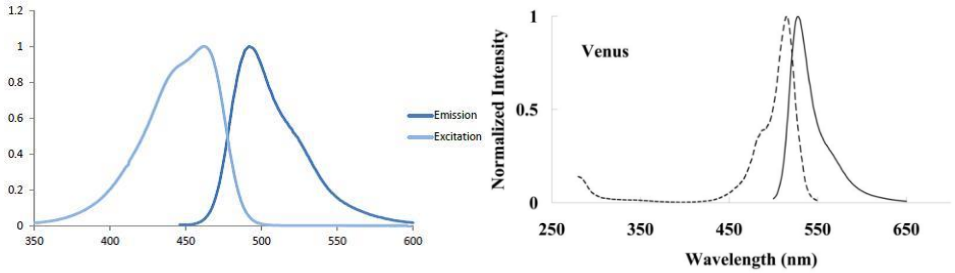

Figure 2. Left: Excitation and emission curves for mTFP with normalized intensity on the y-axis and wavelength (nm) on the x-axis *[27]*. Right: Excitation (dashed line) and emission (full line) curves for Venus *[28]*.

2.3.3 FRET Analysis

To isolate the fluorescence from the two separate chromophores, the light must pass through filters that isolate the appropriate wavelength ranges for one chromophore while blocking out unnecessary wavelengths caused by the other chromophore [1]. As a result, a microscope designed for FRET imaging must contain two filters. There are multiple ways that this problem can be accounted for. The first solution would be to send the light through a beam splitter, which evenly distributes the light two ways. The two paths of light would then be subjected to each filter separately and detected by two separate cameras. The FRET ratio analysis is then conducted based on the ratio between the two separate camera images. Another plausible solution would be to implement a filter swapper that rapidly changes the filter that the light is subjected to. This only requires one camera that would image quickly, and the FRET analysis would occur between two images from the same camera.

There are many professional software applications that are responsible for streamlining the calculation of FRET ratios. These applications use one of several major image processing methods to implement the general protocol associated with obtaining a FRET ratio. Sensitized emission is one of the five general protocols typically used to evaluate a FRET ratio and was the technique the project employed [9]. This general protocol focuses on employing two-channel imaging while implementing software responsible for correcting for crosstalk that may occur between excitation and emission. When fully implemented, this protocol collects five images:

1. Acceptor only taken with acceptor filter set
2. Acceptor only taken with FRET filter set
3. Donor only taken with donor filter set
4. Donor only taken with FRET filter set
5. FRET specimen only taken with FRET filter set [10].

From here, the following calculations are gathered using image processing methods specific to the coding language/imaging package being used:

$$Acceptor\ in\ FRET\ channel\ (Coeff\ A) = \frac{Average\ Acceptor\ Intensity\ using\ FRET\ set}{Average\ Acceptor\ Intensity\ using\ Acceptor\ set}$$

$$Donor\ in\ FRET\ channel\ (Coeff\ B) = \frac{Average\ Donor\ Intensity\ using\ FRET\ set}{Average\ Donor\ Intensity\ using\ Donor\ set}$$

$$FRET\ Efficiency = FRET\ Specimen - (A * FRET\ Specimen\ using\ Acceptor\ filter\ set) - (B * FRET\ Specimen\ using\ Donor\ filter\ set) = \frac{1}{FRET\ Ratio}$$

Using these equations, a user can calculate the FRET efficiency or a FRET ratio of a 'single image'. In an ideal situation, no cross talk would occur in a FRET image, so to obtain the FRET ratio, only the donor and acceptor images are required from the specimen. For this reason, many time lapse software features on FRET microscopes only acquire two images and then implement complex image processing techniques to estimate and subtract crosstalk components, and record a FRET ratio. While this data is not quite as accurate as data collected by other FRET methods, sensitized emission allows users to compile large amounts of data from time lapse studies.

2.3.4 Client Background

Professor Matthew Merrins is an assistant professor in the Biomolecular Chemistry Department with a laboratory under the Department of Medicine at the University of Wisconsin School of Medicine and Public Health. His research is focused on nutrient metabolism in pancreatic islet beta cells using biochemistry, patch clamp electrophysiology, and quantitative imaging. Professor Merrins received his B.A in Chemistry and Biology at Oberlin College and his PhD in Physiology from the University of Michigan. He teaches Human Biochemistry Lab (BMC504) at the University of Wisconsin-Madison. This the class for which an affordable fluorescence microscope is desired.

2.3.5 Competing Designs

There is not a product on the market that meets Professor Merrins design criteria. Most of the educational microscopes have the capability to do fluorescence are not ideal for quantitative imaging. Micrscopes that do have the ability to preform quantitative fluorescence imaging are typically research grade and therefore too expensive for a lab course. The following competing designs meet some aspect of Professor Merrins design criteria, but not all.

The Dino-Lite, as seen in Figure 3, is a small fluorescence microscope that is able to filter a specific wavelength of light [9]. In addition, it can be designed for the different fluorophores used. A Dino-Lite fluorescence microscope can cost between $948-$968 which is dependent upon the type of LEDs needed and emission filters. In addition, software is included and comes with a stand with additional features for adjustments. Even though this device is low-cost, which is what the client requires, this device is not ideal for FRET since FRET requires the use and detection of two fluorophores and their emission wavelengths. As a result, the device would need to be modified to compensate for this.

Figure 3. Dino-Lite Fluorescent Microscope *[9]*. A small handheld microscope that connects to your computer.

As seen in Figure 4 the Lumascope620 uses FRET to image living cells. This microscope is one of the most powerful devices on the market, and has a 5-filter set with 3 exciting filters, 1 triple-band emitting filter, and 1 beam-splitting filter. Utilizing confocal microscopy, one can obtain nanoscale resolution of specimens. In addition, the cells remain alive because this microscope minimizes photobleaching. The microscope also features different configurations of the objective lens, multiple laser options, filters, and detectors [10]. Even though the client would be able to use this microscope for his research, it is too expensive to obtain for a classroom setting because of the microscope's broad capabilities. The team requested a quote of the microscope, and the CEO of Etaluma Inc., Chris Shumate, said it is dependent upon the chassis, filter and lens, illumination source, electronics, and type of camera. According to Nikon, an epi-fluorescent microscope can cost between $50,000 and $125,000. The lower range using manual epi-fluorescent components, on contrary to the most expensive that use an electronic and motorized microscope platform. In addition, the price is impacted on individual components such as the camera, objective lenses, light source, and the types of motorized components used.

Commented [KJ2]: SOURCE

Figure 4. The Lumascope 620 *[10]* is an expensive option that does more than FRET analysis.

The Nightsea converts a stereo microscope into a simple fluorescence system. The product accomplishes this by using an attached filter and an external excitation source. The light source and the filter are assembled to be used with specific fluorophores. The Nightsea comes

with one-color complete setup, modular excitation/emission sets, and a modular white head for a total cost between $1,880-$2,180. Although this device is relatively cheap, this device is not ideal for FRET. This is because FRET uses two fluorophores and would thus require swapping two filters relatively quickly. There is no current data acquisition system as well, which would need to be integrated in the design in order to extract relevant data for determining the FRET ratio [11]. Additionally, as can be seen in Figure 5, the sample is illuminated and detected from above. This can affect the wavelength of the light that reaches the cells and that is detected, skewing the data.

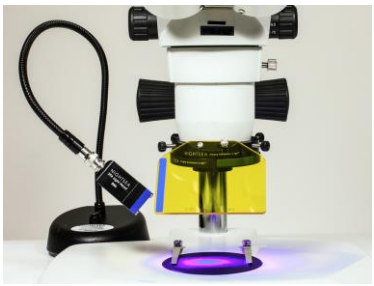

Figure 5. The NightSea Model SFA *[11]* consists of an excitation source and a filter that attaches to stereoscope.

The OPN-Scope (see Figure 6) is a low cost, open source epifluorescence microscope that is used in classrooms and teaching labs in colleges [12]. The first design was built to be added to a compound microscope while a second design was built as a standalone product. This device has two different designs that incorporate 3D printed parts and parts that can be purchased at local hardware stores or from websites like eBay. The six 3D printed parts include an outer shell, drawer that contains the filter cube, handle to pull the drawer in and out, tube to hold the eyepiece and tube to hold the light source. The filter cube holds the excitation and emission filter, along with the dichroic mirror. Some of their materials include: a 2000 lm tactical LED flashlight with a lens for focusing the beam as their excitation source; a Lenovo ThinkPad T430s; a 14-MegaPixel OMAX A3514OU color camera, and ToupView 3.7 software for controlling the time and gain of the OMAX camera. Most of the optical components they acquired were used to control cost.

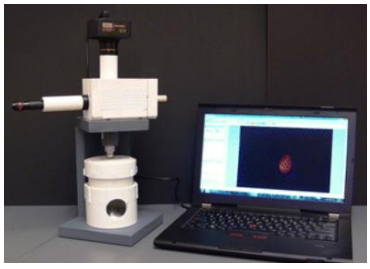

Figure 6. OPN-Scope Open Source Fluorescence Microscope System

2.4. Product Design Specifications

The final product will be a simplified single prototype microscope that will allow the client's students to measure FRET in a classroom setting. This device will be similar to his lab's microscope, as it will contain an excitation source at 430 nm, two different filters for the FRET response (one at 470 nm for the donor emission and the other at 535 nm for the acceptor emission), and a camera. The camera will capture the images of the specimen in the solution chamber and upload them to a compatible computer for image analysis. The goal of the device is to extract accurate acceptor-donor FRET ratios from the images collected. This accuracy does not have to be research-grade, but the microscope should be accurate enough that students can detect a change in lactate expression.

Along with this, the device must be intuitive to use, and the students should have to put in minimal work to obtain the image outputs. The students are not expected to have an extensive microscopy background; therefore, they should have to do little to no image processing. The final product should ideally be under $2,000 so that the lab can purchase at least one device annually with its current budget. To accomplish this goal, most unnecessary/excessive parts of a microscope, such as eyepieces and other components, will be eliminated in this prototype. However, this semester the client expanded the budget to $4,000 for the initial prototype in order that a working prototype is successfully developed. An estimate of the size of the microscope is a 8 inch by 14 inch base with a height less than two feet. If additional software for image analysis is needed, the software used must be free and capable to pair with the microscope to reduce cost. The client requires that the microscope be inverted and that a degree of versatility be present in the design for future applications. A full list of specifications can be found in the PDS in Appendix A.

3. Designs

3.1 Previous Design Work

The design of this miniature microscope for FRET microscopy was started in Spring 2017. During this semester the team had a $2,000 budget, limiting the options for excitation sources and optics. The team considered three cost saving designs (Appendix B.), all of which required the same excitation source. The overall final design is pictured below (Figure 7).

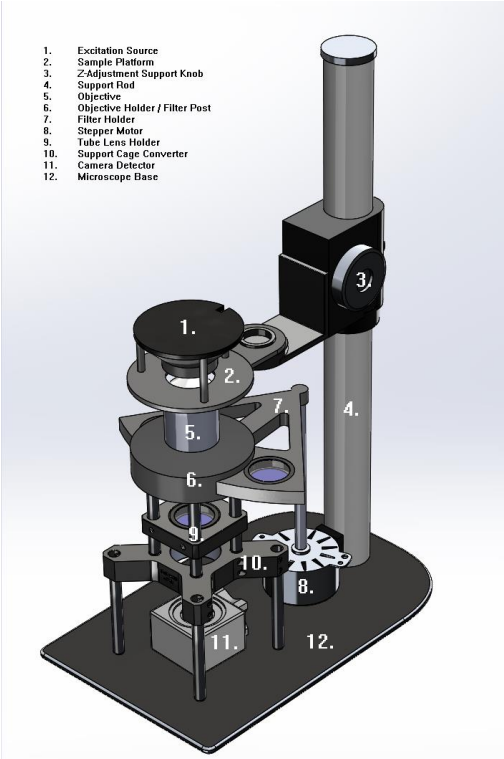

Figure 7. Overview of proposed microscope structure. A legend is included to identify all important components of the design.

Last semester was primarily spent trying to optimize the excitation source, which eliminated the need for a dichroic mirror and an excitation filter, reducing the strain on the budget. The team designed a 430 nm, 10-LED array that sat like a crown over the top of the objective to work as the excitation source. First, a circuit to supply equal amperage at exact time intervals to each LED was devised using a shift register, Arduino UNO, and potentiometer (Appendix C). Next, the team went through a few design iterations for the LED holder, attempting to excite the sample from a crown around the objective (Figure 8).

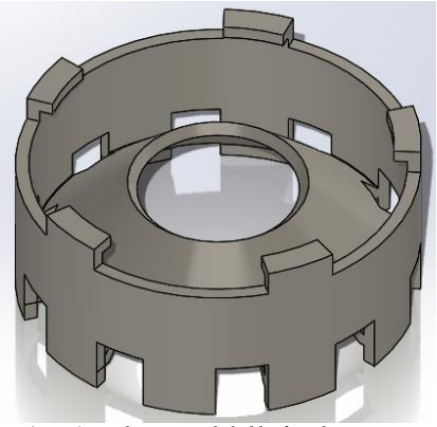

Figure 8. Final LED sample holder from last semester

The LED array was tested with the client's camera (Orca Flash 4.0) as well as the prototype camera (DMK42BUC03 - The Imaging Source). Reasonable results were obtained with the client's camera during the initial testing, but the prototype camera was not sensitive enough to be combined with the prototype excitation source. At a secondary testing with the final LED holder, there was interference from the LED holder in changing the wavelength of excitation light, effectively blocking any signal to the prototype camera or the client's camera. Therefore, the team chose to pursue a different direction for excitation.

One piece of the design that the team hopes to keep or modify for use in the final prototype is the filter-swap mechanism. The design had used a stepper motor, custom semi-circular filter holder, and a filter post in the beam path of the microscope (Figure 9). However, this will be replaced, since the team purchased this mechanism from Thorlabs.

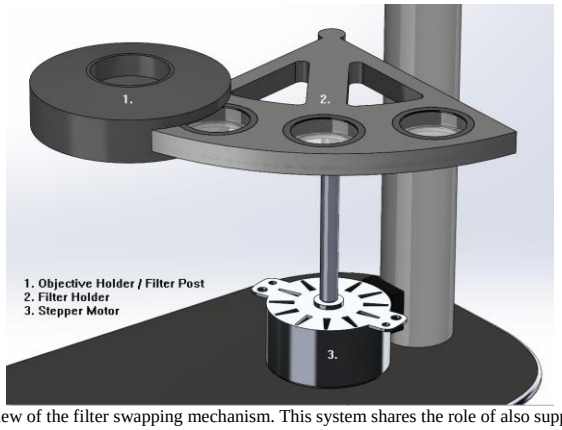

Figure 9. An exploded view of the filter swapping mechanism. This system shares the role of also supporting the objective (not shown). The stepper motor attached to the microscope base will provide the input to switch filters between images.

In the future, the team thinks that we could implement this previous version of our design. A stepper motor with sufficient speed can be used to switch between the 470 nm and 535 nm emission filters accurately, and it can be remotely controlled by experimenters to coincide with excitation illumination and image capture. A custom-printed filter holder will house the needed emission filters and allow fast, compact, and simple swapping of filters by allowing the stepper motor to introduce a small amount of torque that shifts the needed filter into position behind the objective. Movement to the previous filter means that a similar amount of torque is needed in the opposite direction by the stepper motor. In this manner, filter swapping can be accomplished by prompting the stepper motor to rotate in 'positive' and 'negative' directions.

3.2. Initial Design Framework

The team decided on three potential designs for this simplified epi-fluorescent microscope for FRET imaging with various pros and cons. All designs will achieve the same goal of imaging cells expressing Professor Merrins' biosensor as well as outputting a FRET ratio. The designs ideas differ in their mechanical components, software, and mechanism to swap emission filters. All the designs have the same camera, excitation source, optical filters, an objective, and tube lens.

The camera for each design idea will be using is the DMK42BUC03. The camera's specifications can be seen in Appendix D and common camera specifications are defined in Appendix E. The excitation source that will be used is described in section 3.7. Professor Merrins provided optical filters to be used. The objective to be used is Nikon CFI S Fluor 20x. The specifications of the objective are in Appendix F, definitions of objective specifications can be viewed in Appendix G. The tube lens to be used is yet to be determined; however, the tube lens will need to mimic that of Professor Merrins' microscope, the Nikon TI Eclipse [13]. By mimicking the optics of the Nikon TI Eclipse, it can be used as a reference when determining the quality of the prototype. The Nikon TI Eclipse has an internal magnification of 1.5x resulting in overall magnification 30x when a 20x objective is being used. Therefore, a tube lens that provides a magnification of 1.5x will be required.

Commented [KJ3]: Is this still true??

3.2.1 Design One: Thorlabs Assembly

The Thorlabs assembly is the first proposed scope design based on the Design Framework. This scope is assembled with parts that would be purchased from Thorlabs; a company that sells a variety of parts for optical devices. This company is able to provide all necessary parts needed to build a FRET microscope, which creates a high compatibility between parts, while also minimizing compounding error. The potential disadvantages to this scope include the price and the limitations on customization. Thorlabs parts can cost several hundred dollars, which will push the budget near its limit. The scope is also limited based on the parts that Thorlabs sells, so there is little room for creativity from the team with this scope.

3.2.2 Design Two: Artisan Assembly

The artisan assembly is the second considered implementation of the previously defined design framework. The primary objective of this design is to personally manufacture the majority of parts in order to minimize the monetary impact of each part on the budget, and to allow for total customization. While more technical parts such as the camera, excitation source, optical filters, objectives and the tube lens will still be purchased, all mechanical components of the

design including the filter swap would be fabricated by the team. Additionally, software will be developed to control and interface the excitation source, the camera, and compiling the data in a .csv file for the user. As previously mentioned, this kind of autonomy on many aspects of the design permit a much wider scope of design possibilities and customization while utilizing less of the budget, allowing for more expensive optical lenses or cameras to be purchased. Conversely, the fabrication of many parts requires much more expertise and time in comparison to other designs, both limiting resources for this project. Small precision errors in each part are inherent in the process of fabrication, especially when expertise and proper machinery are not available. This compounds with each self-manufactured part included in the design, leaving users with a greater level of uncertainty in the robustness of data gathered, and overall loss of precision in the images collected by the microscope.

3.2.3 Design Three: Combo Assembly

The combo assembly is the third and final design proposed to meet all the requirements of the Design Framework found in section 3.2. This assembly is a combination of the two designs above, in that it takes advantage of some of the parts that Thorlabs offers, in addition to allowing the team to design some of the parts of the microscope. This design creates a compromise on cost; by manufacturing some of the parts instead of buying them from Thorlabs, there will be some budget cuts on the scope. Furthermore, this allows for more creativity and customization with the scope. The disadvantages to this design include concerns with tolerance stacking and scalability. Since there is a combination between Thorlabs parts and fabricated designed parts, there is a risk for tolerance stacking with the scope, leading to less precision. The scope must also have the capability to be manufactured over eight times, which is another potential concern with this assembly.

The combo scope also takes advantage of software that will be written by the team. This software will be focused specifically to run all the tasks necessary for the FRET microscope. This software may be time consuming, however, as there could potentially be a lot of debugging and testing required.

3.3 Design Matrix

After thoroughly researching these three designs, the team created a design matrix to rank them against one another to determine which should be pursued. The team considered five different categories to determine the best option: image quality, manufacturability, cost, operability, and reliability. Considering the advantages and disadvantages of each option, the team collaborated to give each design idea a ranking out of 5 for each component of the design matrix. Design scores highlighted in blue won their category (or tied for the top) and the total highlighted in green is the score for the design idea the team chose.

Table 1 represents the design table matrix for the three different design ideas. The highest scoring design(s) for each respective criterion is highlighted in blue, and the highest scoring design total is highlighted in green.

Criteria (Weight)	ThorLabs Assembly		Artisan Assembly		Combo Assembly	
Image Quality (30)	4/5	24	4/5	24	4/5	24
Manfacturability (20)	5/5	20	3/5	12	4/5	16
Cost (20)	3/5	12	5/5	20	4/5	16
Operability (15)	4/5	12	3/5	9	4/5	12
Reliability (15)	5/5	15	3/5	9	3/5	9
Total (100)		**83**		**74**		**77**

3.4 Design Criteria

Image Quality was selected as the most important design criterion because it is critical that the camera receives enough signal from the fluorophores to create a useful image. This means that the intensity of the donor and acceptor wavelengths should be detectable and small changes will need to be discerned as well. The designs scored equally in this category because all three use the same camera, the DMK42BUC03. This camera was already tested this semester and evaluated. Current tests have proved its ability to detect and discern the two wavelengths, which gave the team confidence that it would work with any of the assemblies considered.

Manufacturability was tied for the second-most design criterion because it is important for the scopes to be easily built and assembled based on the designs. This category considers scalability because the client wishes to ultimately have multiple scopes. This category also considers aligning all the components so that the image is focused onto the detector of the camera as well as the manufacture of any circuitry used to power the design. If there is anything unusual about the stand set-up, it is also included in this category. Thorlabs scored the highest, with a 5/5 because the team would be able to make a list of parts that are purchased from Thorlabs and write a protocol to assemble to scope accordingly. With the other two designs, some manufacturing is required. Since the combo scope still contains some Thorlabs parts, it scored a 4/5, while the completely independent artisan scope scored a 3/5.

Cost was also tied for the second most important design criterion because our client gave us a strict budget, which was doubled to $4,000 for prototyping. The additional flexibility with the budget allows the team to spend more this semester, but it is important to consider that the ultimate goal is to build a scope that costs less than $2,000 since the client wants 8 total scopes. The client's plan is to purchase one or two scopes per year based on this $2,000 budget. However, when evaluating the assemblies this semester, the $4,000 budget was evaluated. The artisan scope scored the highest with a 5/5 because most of the parts would be designed by the team themselves. When purchasing parts from companies like Thorlabs, the prices are oftentimes more expensive because these companies also cover the manufacturing and documenting of the optical pieces. The combo assembly scored second highest with a 4/5 because some of the parts in this design are purchased from Thorlabs. Finally, the Thorlabs assembly scored lowest with a 3/5 because of the priciness of some of the Thorlabs parts.

Operability is meant to quantify user-friendliness of each design. Therefore, the team considered how much image processing would need to be done for each design and whether or

not it would be easy for a student to use. The Thorlabs assembly and the combo assembly both scored the highest at 4/5. These were chosen to have a great operability because they are the easiest scopes for the students to work with. The most significant advantage in operability with this scope is the automatic filter swapper. This would be much more easily controlled when purchased by Thorlabs. Thorlabs also offers its own software, which would likely be easier to use than the team's independently designed software. All three designs require the same image processing due to the optics used.

Reliability is the final design criteria considered because the design should be able to withstand student use for as long as possible. For a cost-effective microscope, ideally the client should not need to purchase new parts or new devices for as long as possible. The Thorlabs scored the highest with a 5/5 because of the quality of the parts that Thorlabs has to offer. The team believes that these professionally manufactured parts will likely be more reliable than parts manufactured by the team. The other two designs scored 3/5 for this reason as well.

3.5 Optics Design

The optics of the design includes choosing an objective, tube lens, and filters. The objective is where light is collected. The choice of objective is influenced by parameters such as magnification, numerical aperture, and material. The tube lens is needed to focus the collimated light onto the sensor, and it is chosen based on parameters such as the focal length and the lens system. The combined specifications of the objective and tube lens determine the spatial resolution, magnification, and field of view. The filters were chosen to collect the most light emitted for the fluorophores while reducing bleed though between the fluorophores as well as bleed through from the excitation source. The goal of the optical design was to mimic Professor Merrins' Nikon TI Eclipse microscope. This would allow for the Nikon TI Eclipse to act as a benchmark for which the prototype could be compared against.

3.5.1 Objective Choice

The ideal objective would have high numerical aperture, 40x magnification, and be a super fluorite objective. The objective would also be an infinite conjugate objective. The difference between an infinite and finite objective are described in Figure 10.

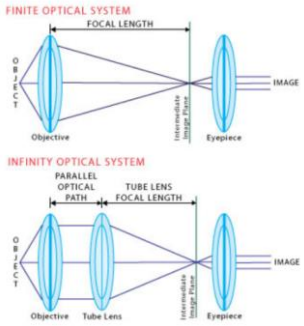

Figure 10. The finite objective does not require lens because the output optical path is not parallel. The advantage of having a parallel optical path is that optical filters can be placed in between the objective and tube lens without effecting the focus of the optical system. Which is why an infinite conjugate objective is desired for this application [14].

The numerical aperture of an objective determines how much light can be collected by the objective and is a unitless measurement. Equation 1 and Figure 11 define what the numerical aperture is. Where n is the refractive index of the medium between the objective and specimen being measured, and μ is the half angle of the aperture angle.

$$Numerical\ Aperature(NA) = nSin(\mu) \quad (1)$$

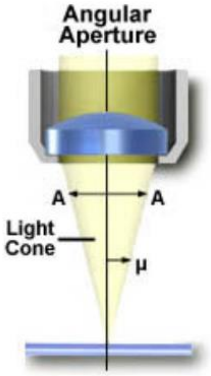

Figure 11. The larger the light cone the more light that can be collected from the specimen. The size of the light cone is determined by the half angle, μ . From the half angle the numerical aperture can be calculated. Typically, the larger the numerical aperture the better [15].

Since the camera being used on the prototype is not as sensitive to light as the Orca Flash 4.0 camera (Appendix H), it is critical to collect as much light as possible to detect the subtle changes in brightness between the fluorophores. The magnification of the objective is determined in conjunction with the tube lens. The relationship is described in Equation 2. Where M_o is the magnification of the objective, F_t is the focal length of the tube lens and F_o is the focal length of the objective [16].

$$Mo = \frac{Ft}{Fo} \quad (2)$$

Typically, objectives are designed for either 160 mm or 200 mm tube lens. Magnification determines the field of view of the optical system (Equation 2). The optimal objective and tube lens pair would maximize the camera's spatial resolution while having an appropriate field of view.

Finally, there are several types of objective such as achromat, fluorite, and apochromatic [17]. The achromatic objectives are the most affordable because the internal lens system is less complicated, and the materials used to manufacture the lenses are less expensive. However, due to the lenses there are significant aberrations when using green light. The fluorite and apochromatic objectives use a material in manufacturing the lens that reduces auto-fluorescence. This especially important when performing fluorescence microscopy. Auto-fluorescence could create unwanted artifacts. Apochromatic are typically the most expensive and corrected for three

different wavelengths, and the fluorite is corrected for two. The ideal objective would be either a fluorite objective or apochromatic objective. Ultimately, Professor Merrins provided a Nikon oil immersed 40x super fluorite 1.3 NA objective free of charge. The fact the objective is oil immersed increases the refractive index, n, (Equation 1) resulting in a high numerical aperture.

3.5.2 Tube Lens

To choose the tube lens, two specifications need to be considered: the type of lens and the focal length. The type of lens will influence the type of optical aberrations that could potentially be present in the image. The three types of lenses considered were a singlet, a doublet, and a triplet lens. The difference between the three is the number of lenses each consist of. A singlet has one, a doublet has two, and a triplet has three. Figure 12 depicts the three types of lenses and illustrates how increasing the number of lenses decreases the optical aberrations.

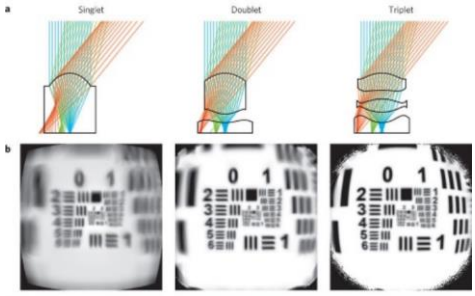

Figure 12. The figure illustrates the typical design of a doublet and triplet lens, row a. Where the doublet consists of a biconvex lens and a concave lens. The triplet consists of different types lenses based on its application. Row b of the figure illustrates the decrease in aberrations as the number of lenses increases [18].

The doublet lens was recommended by Professor Rogers, and it is also widely used in microscopes. In addition, there are no triplet lenses of the desired focal length.

The focal length of the tube lens was chosen to satisfy the Nyquist theorem. The Nyquist theorem states that in order for a signal to be properly resolved, the signal be must be sampled at twice its frequency [19]. Thus, the projected size of the object should be sampled twice it's frequency. This is described in Equation 3.

$$Projected\ Size = 2 * pixel\ size \quad (3)$$

The projected size based on the optical system is described in Equation 4 where magnitude is derived from Equation 2 and where r is spatial resolution and is defined in Equation 5. Resolution, r, is determined by wavelength, λ, in micrometers, and numerical aperture, defined by Equation 1.

$$Projected\ Size = Mo * r \quad (4)$$

$$r = 0.61 * \frac{\lambda}{NA} \qquad (5)$$

The numerical aperture, pixel size, and wavelength is already known and the focal length of the objective F_o can be derived since it is known that Nikon objectives are designed for a tube lens of 200 mm (Equation 6).

$$5mm = \frac{200mm}{40} \qquad (6)$$

Thus Equations 3 through 5 can be rewritten to solve for the focal length of the tube lens in Equation 7.

$$\frac{2*pixel\ size*Fo*NA}{0.61*\lambda} = Ft \qquad (7)$$

$$\frac{2*3.5\mu m*5mm*1.3}{0.61*0.47\mu m} = 158.702\ mm \qquad (7.1)$$

$$\frac{2*3.5\mu m*5mm*1.3}{0.61*0.535\mu m} = 139.420\ mm \qquad (7.2)$$

This equation is used twice because there are two different wavelengths. By plugging in the known values, it is determined the tube lens optimized for spatial resolution would have a focal length between 139.420 mm and 158.702 mm. Taking the average of the two results in a tube lens length of 149.061. Typically, there are not 149 mm tube lenses on the market; however, there are 150 mm tube lens available.

The spatial resolution should not be the only decision in determining the correct lens. Another important calculation is the field of view. The field of view is defined as the total observable area, and it is a function of the magnification of the system and the size of the sensor. Equation 8 describes the field of view where M_o is the magnification calculated from Equation 2. Height and width represent the dimension of the field of view. The X does not represent multiplication, but rather dimensions of the field of view [20].

$$Height\ X\ Width = \frac{Camera\ Sensor\ Height}{Mo}\ X\ \frac{Camera\ Sensor\ Width}{Mo} \qquad (8)$$

Because the current specimen being used to test the microscope are pancreatic islet cells, it is important to have a large enough field of view to see an entire islet. Mammalian islets are typically between 100 µm to 200 µm in diameter [21]. Using Eq. 8 and Eq. 2 the field of view of a 100-mm tube lens and a 150-mm tube lens is calculated. See Appendix D for camera specifications.

$$\frac{4.8mm}{100mm/5mm}\ X\ \frac{3.6mm}{100mm/5mm} = 0.24mm\ X\ 0.18mm \qquad (8.1)$$

$$\frac{4.8mm}{150mm/5mm} X \frac{3.6mm}{150/5mm} = 0.16mm\ X\ 0.12mm \qquad (8.2)$$

Because the 100mm tube lens provides a larger field view, it was chosen as the tube lens. This will allow the prototype microscope to image islet cells and compare fluorescent measurements with the Nikon TI Eclipse. In the future, when the microscope is used to image yeast, which are much smaller, it would be better to switch to the 150mm lens to increase spatial resolution.

3.5.3 Filters

Two sets of filters and a dichroic mirror are need typically needed for epi-fluorescence microscopy. The first set of filters are known as the excitation filters. The excitation filter is used to filter the light emitted from the excitation source. This ensures the fluorophores are excited at the correct wavelength and prevents unwanted light from being detected. In this application 430-nm wavelength of light is needed to excite the mTFP fluorophore (Figure 13). Please note that Professor Merrins uses mTFP, a variant of CFP, and Venus, a variant of YFP. CFP is used as an estimate for mTFP for the figures in this section and YFP is used for Venus.

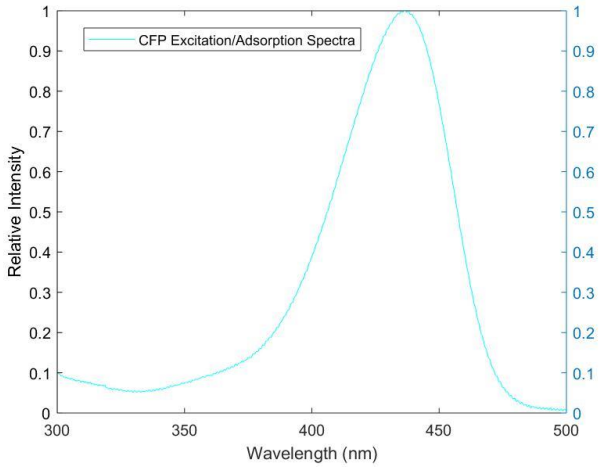

Figure 13. The excitation/adsorption for CFP. A light source centered at 430 nm would lead to the CFP emitting the most light [22].

The second set of filters needed are emission filters. Emission filters are needed to ensure only the light emitted by the fluorophores is detected by the sensor. For this application the wavelengths of light being detected are centered near 480nm and 535nm (Figure 14). In addition to the emission filters a dichroic mirror is needed. The dichroic mirror allows for excitation and imagining in the same channel.

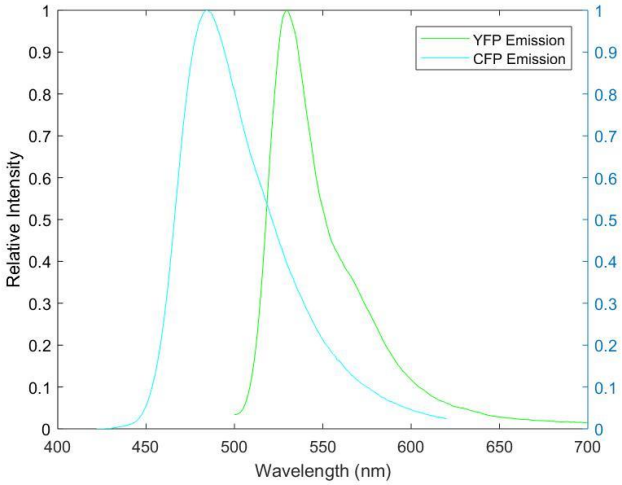

Figure 14. Emission Spectra CFP, in cyan, and YFP, in green. CFP is centered around 485nm and YFP is centered around 535nm [22].

The excitation filter chosen was provided by Professor Merrins. This was chosen because it prevents light over 445 nm from entering the imaging path; therefore, it prevents undesired light from entering the imaging path (Figure 15).

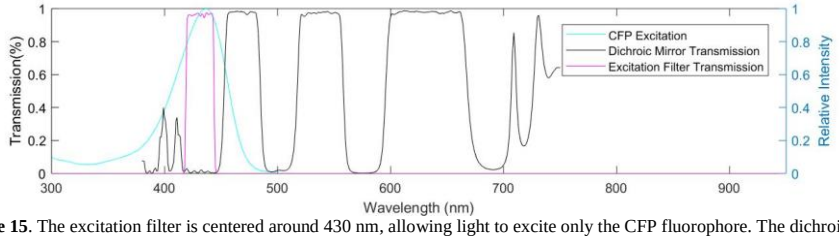

Figure 15. The excitation filter is centered around 430 nm, allowing light to excite only the CFP fluorophore. The dichroic mirror allows only the emission from the fluorophores and not light from the excitation source [22].

The dichroic mirror chosen is a triple pass band pass filter (Figure 16). The dichroic mirror was provided by the client and was chosen because it reflects the light allowed through by the excitation filter, while passing through only the light emitted by the fluorophores (Figure 16). This prevents 430 nm light from bleeding through to the detector and corrupting the image. The emitted filters were also provided by the client and were chosen to maximize the light captured by the individual fluorophores, CFP and YFP, while reducing the cross talk between the light emitted by the fluorophores (Figure 16).

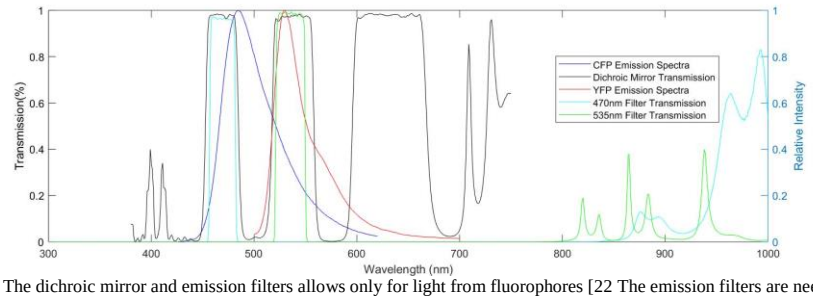

Figure 16. The dichroic mirror and emission filters allows only for light from fluorophores [22 The emission filters are needed to isolate the light from CFP and YFP].

Cross talk is when light emitted by the CFP fluorophore overlaps with light emitted by YFP. When attempting to only image the light emitted by the YFP, there is also light present from the CFP; therefore, the YFP signal is not perfectly isolated.

3.6 Power and Control of Excitation Source

The team chose to use three Vollong, 3W high power LEDs held in parallel to excite the sample. These LED's operate with a forward voltage of 3.6 V at 750 mA [23]. These LEDs are held in series with 5Ω/3W resistors that can work efficiently in the power range. Each LED provides 200 lumens of light, for a total of 600 lumens. The circuit is controlled by an Arduino microcontroller which opens and closes an npn BJT transistor and also supplies 5V to the collector side of the BJT. When the Arduino switches "on", the transistor is powered and enters the active region, such that the circuit can run. When the Arduino switches "off", the transistor does not receive power and thus the LEDs will be turned off. Furthermore, the potentiometer located on the emitter side of the BJT is used to control the current on the collector side of the device. This allows for the LEDs to supply a range of brightness based on the resistance set by the potentiometer. These approximations are based on the formulas provided in 9.1 and 9.2 [24].

$$I_e = \frac{V_e}{R_e} \; ; \; I_e \cong I_c \qquad (9.1)$$

$$I_c = \frac{V_b - 0.6}{R_e} \qquad (9.2)$$

where V_b is 3.3 V and R_e depends on the potentiometers resistance.

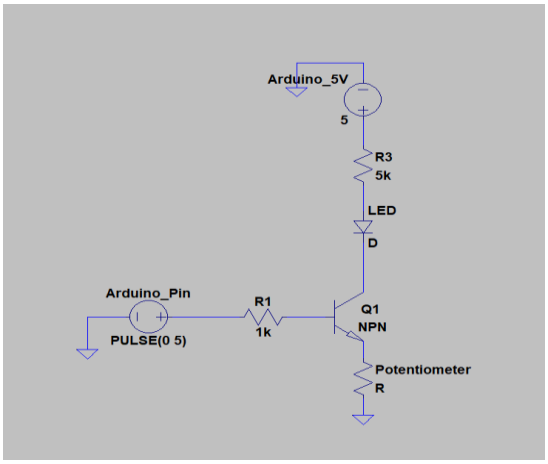

Figure 17. The final circuit schematic developed in LTSpice. The LED is in series with a resistor to provide the appropriate voltage from the Arduino. The BJT transistor controls the ON/OFF switch. The potentiometer controls the current flow through the LED.

In Figure 17, the Arduino is modeled by a Pulse Signal, which fluctuates between 3.3V on period and a 0V off period. The three LED's are represented by diodes with a forward voltage of 3.6 V. The Arduino allows supplies 5V source voltage to the LEDs. The potentiometer is found on the collector side of the BJT, which represents a range of resistances.

The high-powered LED is connected to a 40.6 mm x 40.6 mm heat sink to help dissipate the heat in generates while providing light. This heat sink is an aluminum model, which dissipates heat so that the LED can run longer without the risk of damage to the LED or the circuit [25]. By arranging the thermal dissipation equation (Equation 10), the maximum power that the device can dissipate can be determined.

$$\Delta T = \theta_{J-A} * P_D \qquad (10)$$

The client has also provided the team with a Sutter Instruments TLED system to provide excitation for the system. The TLED provides 430 nm high power LED light at a forward voltage of 6 V. This LED system is controllable manually via a toggle switch or through a TTL connection to a computer [25]. This system is advantageous in that it can be connected directly to the microscope because it is built by Sutter Instruments. However, this TLED system adds a significant amount of cost to our system, which must be considered with scalability of the device. The TLED system is currently listed at $1,975 [25].

These two systems can be compared to the client's $100,000 microscope based on the brightness the light source provides. The SOLA light source that client's microscope uses is capable of providing 750 lumens of light at 100% output [26]. This is comparable to the proposed circuit design, which can provide 600 lumens. Additionally, during testing, the team did not need more than a 50% output from the client's microscope. The exact CREE LED used in the TLED scope is unknown; however, most CREE XHP-50 LEDs can provide at least 700 lumens of light. This makes the TLED comparable to the SOLA as well. The microscope will be

tested with both light sources, to test the quality of the proposed microscope in consideration for scalability of the microscope next semester.

3.7 Mechanics

3.7.1 Mirror Cubes

For the first prototype, the team decided to incorporate a dichroic mirror, which allows light of a specific wavelength to pass and reflects light of other wavelengths. The dichroic mirror was inserted inside a black cube to reduce auto-fluorescence of the physical components. The filter cube should meet the following criteria: allow easy access to the dichroic mirror, one 25 mm hole for the cage mount with the excitation filter, and one 25 mm hole for the objective. The cube must also allow cage rods so that the cube can be mounted to the cage plate and the microscope can be fully assembled.

After making the first prototype of the microscope using Thorlabs parts, the microscope was functional, although taller than anticipated. To condense the height of the microscope, the team decided to purchase a fold mirror. This mirror would be inserted in a cube below the dichroic filter cube. As light is emitted from the cells, it passes through the dichroic mirror, and reflects off the fold mirror to the camera that is attached to the side of the filter cube.

A typical filter cube on Thorlabs can cost over $300. As a result, the team decided to fabricate a customized dichroic filter cube, in addition to a cube for the fold mirror, by using SOLIDWORKS and 3D printing the design. Figure 19 shows the stackable cubes that slide into each other through a slot made on the cube.

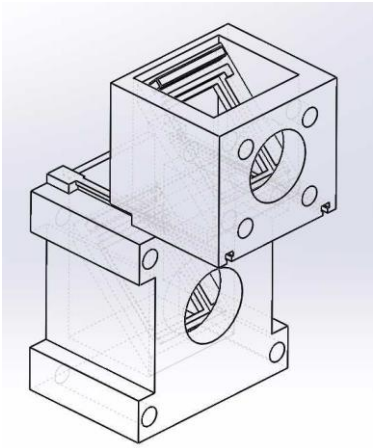

Figure 19. SOLIDWORKS design of dichroic and fold mirror filter cube. The top dichroic filter cube is enclosed with a top that has a 26 mm hole in order to attach the objective lens which is be directed under the cells. The center and outside holes were dimension

Both cubes contain a holder, as seen in Figure 20, for the mirror with a handle. Both mirrors fall at a 45-degree angle inside the cube. If needed, both cubes can be disassembled, and the mirrors can be removed.

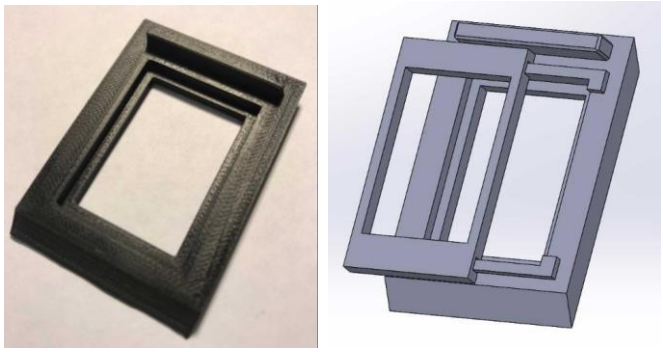

Figure 20. Dichroic and fold mirror holder. The 3D printed holder allows both mirrors to fit securely inside the holder. The top extrude section of the holder allows the mirrors to be taken out of the cube. The holder and filter cube were dimensioned to fall at 45 degree angles inside the cubes.

3.7.2 Light Source Mount

The light source is connected to a 40.6 mm x 40.6 mm heat sink mounted on a 3D printed tube as seen in Figure 21. The high-powered LED is attached to the heat sink using a thermal glue that improves the heat dissipation of the LED. The 3D-printed tube was designed to enclose the light being emitted. The tube is connected to the cage plate that contains the excitation filter, which is attached to the dichroic filter cube.

Figure 21. 3D-Printed light source tube. This tube connects the light source that is attached to the heat sink. The dimensions align to the size of the cage plate that contains the emission filter inside, which will all be attached to the side of the dichroic filter cube.

3.7.3 Z-Adjustment

The team brainstormed three potential ideas for the z-axis adjustment of the microscope. The three designs were a PVC pipe with chemistry stand, 3D printed rack and pinion, and a purchased z-axis adjustment. The z-axis was critical to the design of the microscope to allow the students running experiments with the microscope to focus the specimen. In addition, the adjustment had to be precise enough to ensure that the images captured of the cells are focused. A design matrix (Table 2) was made to determine the optimal z-axis adjustment option.

Table 2. Z-axis adjustment design matrix. A design was made to access three options for the z-axis adjustment. The designs were ranked according to four important criteria: manufacturability, accuracy of adjustment, easy of adjustment, and cost. The sections highlighted in blue are the highest ranked in that categories, whereas the highlighted green section is overall highest scored design.

Criteria (Weight)	PVC Pipe with Chemistry Stand		3D Printed Rack and Pinion		Stereo Microscope Focusing Rack	
Manufacturability (30)	3/5	18	4/5	24	5/5	30
Accuracy of adjustment (30)	3/5	18	3/5	18	4/5	24
Ease of adjustment (20)	3/5	12	4/5	16	5/5	30
Cost (20)	5/5	20	4/5	16	2/5	8
Total (100)	**68**		**74**		**92**	

Manufacturability is an important criterion for the client since he would like to eventually reproduce the design to make several microscopes. Since the client does not have access to machining equipment and has limited time, it is important to consider how difficult it would be to fabricate the part. The PVC pipe design would be the most difficult to manufacture since a PVC pipe and chemistry stand would need to be purchased. In addition, the pipe would have to be adjusted properly over the cells. The 3D printed z-axis would be easy to fabricate as long as the client has access to a 3D printer. The best alternative was the stereo microscope focusing rack since it could be bought and easily attached to a stand.

Accuracy of adjustment is important to obtain a clear image of the cells. The PVC design would be the least accurate since the chemistry stand would have to be adjusted by hand, clamped, and then adjusted with the PVC pipe. The 3D printed rack and pinion worked well, adjusting in the z-axis, but still was not as fine of an adjustment as a metal or aluminum rack and pinion is as seen on the purchased stereo focusing rack.

Ease of adjustment is critical for the students to ensure that they will be able to focus on the cells without difficulty. The PVC pipe has an adjustment for the chemistry clamp in addition to the fine focus from the PVC pipe. Since the PVC pipe is threaded, the current design does not prevent the dish of cells from rotating. The 3D printed design and stereo adjustment both have rack and pinions for z-axis adjustment, which keeps the cells stationary during focusing. The 3D printed rack and pinion was ranked lower than the stereo focusing rack since the material would occasionally catch on the side of the gear, whereas the aluminum rack and pinion allowed a smoother adjustment.

Cost was ranked the lowest the categories since the ideal criteria for the z-axis adjustment was to be able to be easily reproduced, and allow the best precision adjustment to attain a clear image. The PVC was ranked the cheapest since PVC piping and a chemistry stand is inexpensive. The 3D printed rack and pinion requires the cost of the materials to print, which varies around the type of material chosen. If using Nylon and PVA for the supports, the overall system should cost under $30.00. The stereo focusing rack was the most expensive because it is manufactured by a company. These devices can vary in cost depending on the company.

3.7.4 Optical Breadboard/Base

The team decided to manufacture an optical breadboard to improve the portability and modularity of the microscope as well as to hold the components securely in place. The board was manufactured out of a piece of 8" x 14" aluminum with a 3/8” width. To attach and move each component of the device, the board was milled with 1/4" holes that were 1" spaced apart and 1/2"

from the edges of the board. Because the board is not very thick, it will still need to be raised. Additionally, the team plans on adding components to the board to better damp vibrations that could impair image quality.

3.8 Software

3.8.1 Image Analysis

To begin development of image analysis features in the software of the project, a script performing a basic FRET ratio estimate was created in MATLAB. This code operated by simply entering the file directory path of the mTFP and Venus images (note these variables are simply referred to as CFP and YFP respectively in the code) of the same specimen taken at roughly the same time. These images were then processed into three-dimensional arrays, representing the x-location, y-location, and pixel value of each pixel in each respective image. From here, a threshold was applied to the images to negate the influence of background pixels that experienced little or no change in brightness between images. The pixels of interest were then divided, and their specific ratios were stored in an image/array. To obtain an overall average ratio for the specific image series (mTFP and Venus images), the values in the divided image/array from the previous step were all averaged into a single averaged ratio, representing an estimate of the FRET ratio of the image. It is important to note that while this method gives a solid estimation of the FRET ratio of the image, there were no image processing techniques utilized to estimate and eliminate cross talk between acceptor and donor molecules, detracting some of the accuracy of this estimate (when compared to professional software). This general algorithm has been outlined in Figure 22.

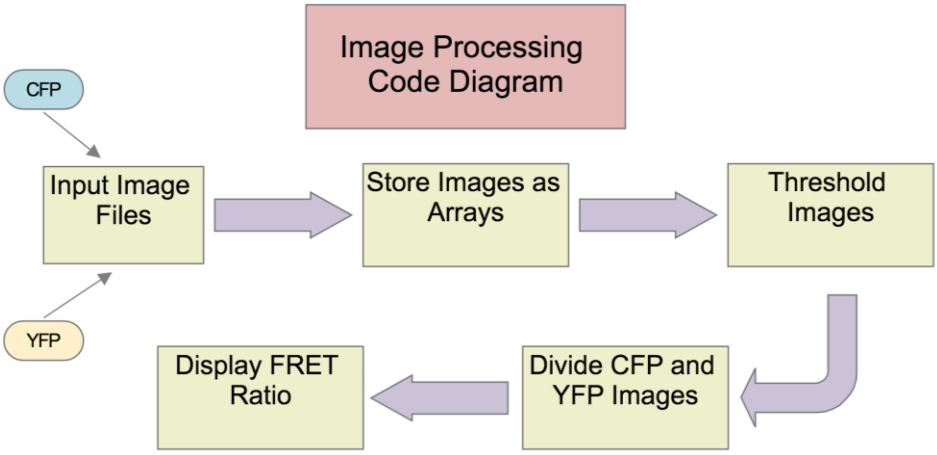

Figure 22. Block diagram covering general protocol of image analysis in software.

After the MATLAB code was developed, the general skeleton was implemented in C# extending the EmguCV (a C# wrapper for Open CV) image processing package. This was done to streamline the use of image analysis with the microscope control GUI into a single, comprehensible application. The general protocol for image analysis, as coded in MATLAB, was implemented in the ImageProcess() method of the GUI code as displayed in Appendix J. This method is run a single time when the 'Calculate FRET Ratio' button on the GUI is selected, shown in Appendix L, and is run 120 times when the time lapse feature is selected on the GUI. When the time lapse feature is run, an array is created to store the FRET ratios for each pair of images which can then be used by the user to create graphs or further analyze independently or with an application such as Microsoft Excel.

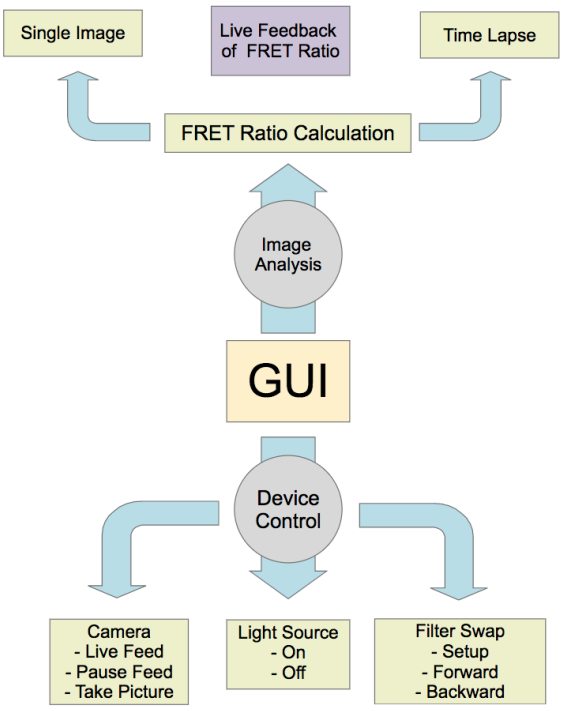

Figure 23. Schematic overviewing the functionality of microscope GUI.

3.8.2 Filter Swap and System Controls

The GUI software was written in Microsoft Visual Studio using C# through a Windows Forms Application. The enabled functions of the GUI are schematized in Figure 23. The GUI was able to control the LED light source and the filter swapper connected to the Arduino through Serial communication with the Arduino microcontroller. The application sends a bit number to the microcontroller based on which button the user selects, and this number is subjected to a case

statement to determine a response from either the filter swapper or the LED. The user can choose between the two filters needed for the FRET analysis, and furthermore, the user can calibrate the device to the appropriate starting filter. The user can also turn the LED source on and off. If the user chooses to select a time lapse analysis, the GUI code communicates with the Arduino based on the conditions set in the TimeLapse() method code. The DMK42BUC03 camera was controlled directly through the implementation of the device's SDK and importation of The Imaging Control library as a reference into Visual Studio. From here, an imaging device object was created, inheriting the Imaging Control library features. Buttons were created to allow for live feed from the camera, a stoppage of the live feed, and taking a single picture with the camera.

3.9 Final Assembly and Design

In the initial design matrix, the Thorlabs assembly was ranked as the top design. During the initial porotype fabrication, the team decide to assemble a functional microscope in Professor Roger's lab using parts from Thorlabs and Edmund Optics. Throughout the design, the team decided to purchase the corresponding parts. In addition to ordering parts, the team decided to 3D print a dichroic and fold mirror filter cube to decrease the cost of the microscope.

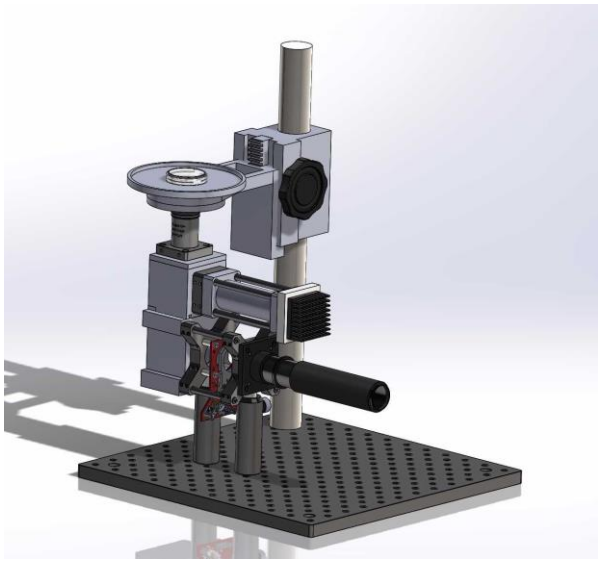

Figure 24. Final SOLIDWORKS assembly of FRET microscope. The final assembly has three 3D printed parts: dichroic and fold mirror cubes, mirror holders and tube for light source. The additional parts assembled were purchased from various optic suppliers. The microscope contains an adjustable z-axis that will enable the user to attain a clear image of the cells. The top filter cube holds the dichroic mirror whereas the bottom filter cube holds the fold mirror. The microscope will be secured on an optical board.

The prototype features a 3W white high-power LED that is attached to a heat sink. The light source is mounted onto a 3D printed tube to ensure no light is lost to the environment and that the user of the microscope will not be exposed to it. As the light travels through the tube it will pass through an excitation filter that allows 430 nm wavelengths to pass through. The top filter cube holds the dichroic mirror at a 45-degree angle, which will reflect the light up to the cells. As the light hits the cells, the cells will fluoresce and emit lower energy wavelengths. The donor fluoresces at 470 nm, which will excite the nearby acceptor fluorophore Venus, which fluoresces at 535nm. The light emitted can pass through the dichroic mirror to the filter cube below which holds a fold mirror at a 45-degree angle. A filter-swap is connected to the fold mirror cube that contains two emission filters; one at 470 nm for the donor emission and one at 535 nm for the acceptor emission. The design will enable the device to obtain an acceptor-donor FRET ratio by capturing the two images back-to-back while the emission filter switches. The filter-swap is attached to a tube lens that is c-mounted onto the camera.

The camera will be connected directly to the user's computer along with an Arduino microprocessor. The Arduino microprocessor will include connections from both the high-powered LED and the filter-swap. This will connect all GUI-controlled components to a computer, which will be running the GUI software. This will permit complete control of the microscope as well as allowing the user to compile image analysis information.

4. Experimental Set-up

4.1 Previous Experiments

To understand the experimental setup of the project this semester, it is necessary to understand the testing and results from the previous semester. In preliminary testing, the team compared the LED-array excitation source with the Lumencor SOLA of the client as well as the prototype camera with the ORCA-Flash 4.0. This testing showed that the prototype camera could detect the biosensor with the Lumencor SOLA, and the ORCA-Flash 4.0 could detect the biosensor with the prototype camera at 535 nm. However, the ORCA-Flash 4.0 could not detect the biosensor at 470 nm, and the combination of the prototype camera and LED array proved ineffective at detecting the biosensor at either wavelength.

4.2 Experimental Overview

4.2.1 Preliminary Camera Experimentation

The BME design team decided to do a quantitative comparison of FRET detection of the current camera purchased (DMK42BUC03) compared to the client's camera (ORCA-Flash 4.0). This test was performed to determine if there was difference of the detection of FRET between the two cameras, and it was meant to confirm whether the DMK42BUC03 could be used for accurate FRET results. As a result, both cameras were attached to the client's microscope, and the same FRET protocol was performed.

Throughout the experiment, pancreatic islet cells were used, and the software Nikon Elements was used to control the microscope and light exposure. Images from the purchased camera were taken using IC Capture. Images were taken using a 40x objective lens. The goal of

this experiment was to determine if the camera purchased would be able to detect the FRET efficiency when subjected to high and low concentrations of glucose. Therefore, the client's camera was used as the control which would later be compared to the FRET efficiency obtained from the purchased camera.

Testing with the 40x objective lens showed that the field of view was extremely small using the prototype camera. In an actual experiment that biochemistry students will be doing, they will be using yeast cells which will be much smaller than islets, so this would likely be fine for the desired application. However, to compare the images, a second experiment was completed using a 20x objective lens, resulting in images that were analyzable.

At this time, an additional time-lapse experiment was performed. With no light exposure, the pancreatic islet cells were first subjected to a high concentration of glucose (16.7 mM) for a duration of 10 minutes. During the high glucose wash, a time-lapse was used to detect the FRET ratio over time. Every six seconds, two images were captured, and the two emission filters were switched out instantly. A 20X objective lens was used for the remainder of the experiments. Once the cells were washed for approximately ten minutes, the time-lapse was stopped, and a variety of images were captured. A selection of these photos of the time-lapse were chosen to be representative of all the images.

4.2.2 Comparison of Imaging Algorithms

To evaluate the efficacy of the imaging algorithm, testing was done to ensure that it performed similarly to professional software. A basic experiment was performed using the Nikon TI Eclipse microscope in which a colony of pancreatic islet cells were exposed to varying levels of glucose concentration. While the concentration of glucose slowly increased/decreased (varied based on the trial), time lapse images were taken and saved by the Nikon software. These images were then analyzed directly by the Nikon software, producing FRET ratios over a specified time scale. The same images were then analyzed using the image processing algorithm developed in MATLAB to produce FRET ratios (unique to the imaging algorithm) of the same images. This data was then saved for later statistical testing.

4.2.3 Determining the Spatial Resolution

To determine the spatial resolution of the optical system, a 1951 USAF resolution test chart was imaged. The test chart consists of bars of standard size and spacing and is used in industry to determine the resolving capabilities of optical systems. The test chart consists of 9 groups ranging from -2 to 7. Each group contain six elements and each of the six elements consist of 3 horizontal and 3 vertical bars. The team imaged the chart with a 40x 0.65NA objective, 100mm tube lens and the DMK42BUC03 camera from The Imaging Source. The team chose this objective because the objective to be used in the final design was unavailable; therefore, the team used the next best available option. The team calculated the diffraction limited resolution and determined the experimental resolution from the test chart.

5. Results and Discussion

5.1 Previous Conclusions

The team performed a two-tailed t-test to compare the client's camera with the prototype camera using the client's excitation source, lenses, and filters at 535 nm. This test was performed on Figures 25A and 25B. Because the team needed to move the apparatus to insert the prototype

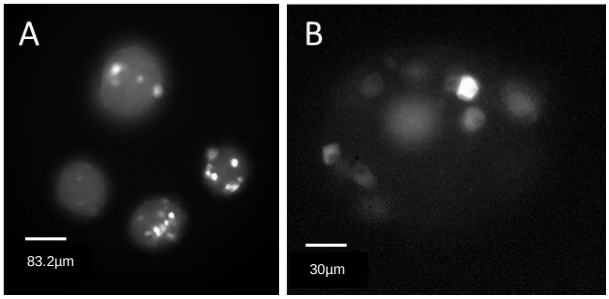

Figure 25. Images from past semester at 535 nm. (A.) Image taken with Lumencor SOLA and Flash4.0 (B.) Image taken with DMK42BUC03

excitation source, the images were not taken at the same spot. Therefore, the team chose to compare the four brightest spots in one of the colonies. The colony to the far right of Figure 25A was used in analysis. First, an average background intensity was found for each image using FIJI over an area in the corner of each image. Then, the average intensity for each of the four brightest spots was computed by tracing around the outside of the spots. Then, these four intensities for each image were compared in a ratio to the average background of that image. This resulted in ratios ranging from 5 to 20 for each of the spots. Then, these ratios were listed in order of highest to lowest for each photo. This way the brightest spots were compared to each other, then the second brightest, and so on. Using a two-tailed, paired t-test, the team computed a p-value of 0.204 and a 95% confidence interval of -14.86 to 4.83 (Table 3).

Table 3. Comparison of four brightest colonies using photos taken by the prototype and clients camera to image each picture at 535 nm.

Prototype vs. Client Camera	
p-value	0.2036
95% CI	(-14.86,4.83)
t	1.6205

Based on these statistics, it appeared that there was no significant difference between the prototype camera and our client's camera in their ability to detect the biosensor fluorescence from the background. Since the microscope will only need to detect fluorescence intensity, overall image quality does not need to be evaluated.

5.2 Results

5.2.1 Image Acquisition

The images were first captured with the client's camera using the 470 nm and 535 nm emission filters, and the client's excitation source, the Lumencor SOLA. One image was captured for each emission filter; one image using 10% SOLA and one image using 50% SOLA. The team first took images at high glucose with the DMK42BUC03 and the 20x objective. Since initial images taken at 10% SOLA showed that the camera was not able to detect the islets (Figures 26A and 26C) the SOLA was increased to 50%, where it appeared that the islets could be detected for each of the desired wavelengths (Figure 26B and 26D).

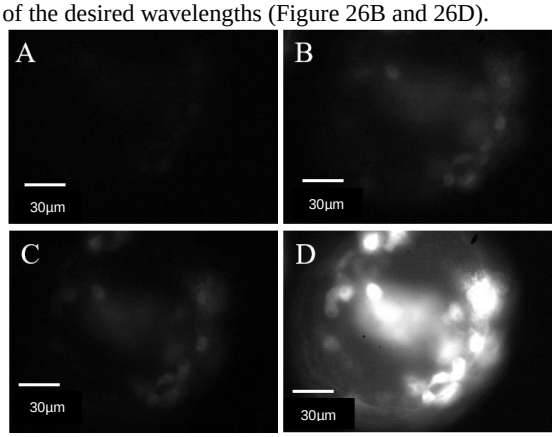

Figure 26. Fluorescence microscope images at high glucose concentration with 20x objective and DMK42BUC03. (A.) 470 nm emission filter with 10% SOLA (B.) 470 nm emission filter with 50% SOLA (C.) 535 nm emission filter with 10% SOLA (D.) 535 nm emission filter with 50% SOLA

After images were obtained using the DMK42BUC03, the team captured more images using the client's camera at high glucose. The same objective, excitation intensities and emission filters were used, starting with a 10% SOLA (Figures 27A and 27C), but they were also imaged at 50% SOLA (Figures 27B and 27D). The image taken at 535 nm appeared to saturate, however, indicating a lower SOLA power would be required.

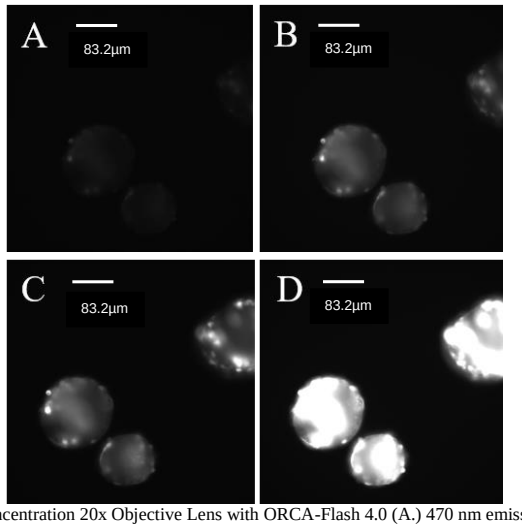

Figure 27. High Glucose Concentration 20x Objective Lens with ORCA-Flash 4.0 (A.) 470 nm emission filter with 10% SOLA (B.) 470 nm emission filter with 50% SOLA (C.) 535 nm emission filter with 10% SOLA (D.) 535 nm emission filter with 50% SOLA.

After all images were obtained, the time-lapse was started, and low glucose concentration (2 mM) was added over a period of 10 minutes, taking photos with the Orca Flash 4.0 and 20x objective during the transition. Then, photos were taken at low glucose with the DMK42BUC03 and 20x objective, using both 10% SOLA (Figures 28A and 28C) as well as 50% SOLA (Figures 28B and 28D) for the experiment. It clearly showed that 50% SOLA is the better option for imaging the cells, and it also demonstrated that a higher intensity would not necessarily be needed for the team's prototype.

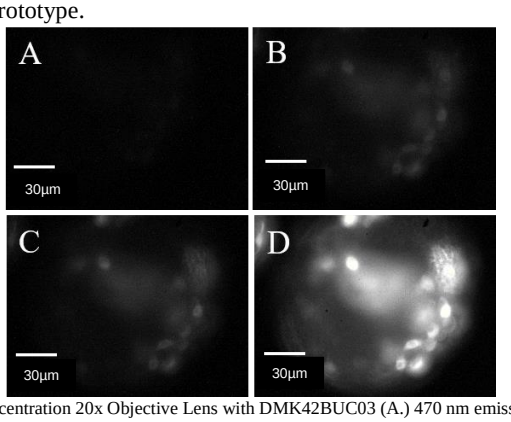

Figure 28. Low Glucose Concentration 20x Objective Lens with DMK42BUC03 (A.) 470 nm emission filter with 10% SOLA. (B.) 470 emission filter with 50% SOLA. (C.) 535 emission filter with 10% SOLA. (D.) 535 emission filter with 50% SOLA.

Finally, low glucose images were taken with the Orca Flash 4.0 and the 20x objective lens. These showed that for the client's microscope 50% SOLA (Figures 29B and 29D) saturates

the image taken at 535 nm (Figure 29D). However, 10% SOLA (Figures 29A and 29C) did not appear bright enough; therefore, the ideal brightness is likely somewhere in-between to compromise between the low 470 nm fluorescence and the high 535 nm fluorescence, something the prototype microscope will need to keep in mind as well.

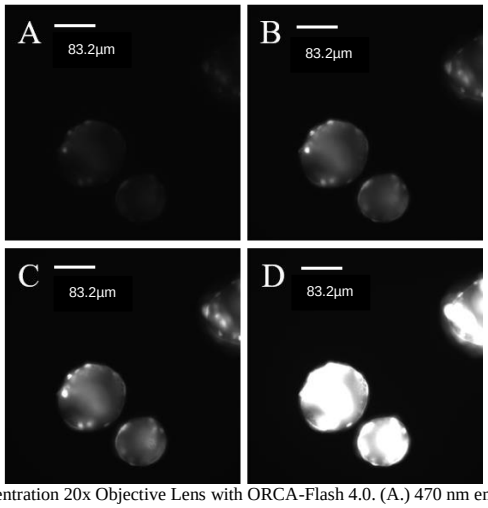

Figure 29. Low Glucose Concentration 20x Objective Lens with ORCA-Flash 4.0. (A.) 470 nm emission filter with 10% SOLA. (B.) 470 emission filter with 50% SOLA. (C.) 535 emission filter with 10% SOLA. (D.) 535 emission filter with 50% SOLA.

The team also imaged the islets using the client's ORCA-Flash 4.0 and the 40x objective to get a similar field of view as when using the 20x objective with the prototype camera. These images showed that at 50% SOLA and 535 nm (Figures 30D and 31D) there are no discernable islets. Even at 10% (Figures 30C and 31C) the camera blurs the islets together. This shows that perhaps by increasing the magnification of the prototype scope the team will not need to worry about using such a bright excitation source.

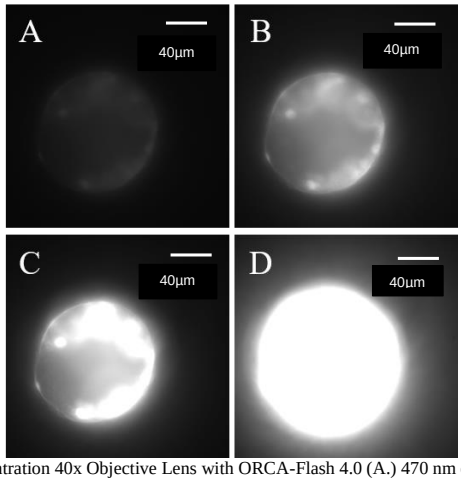

Figure 30. High Glucose Concentration 40x Objective Lens with ORCA-Flash 4.0 (A.) 470 nm emission filter with 10% SOLA. (B.) 470 emission filter with 50% SOLA. (C.) 535 emission filter with 10% SOLA. (D.) 535 emission filter with 50% SOLA.

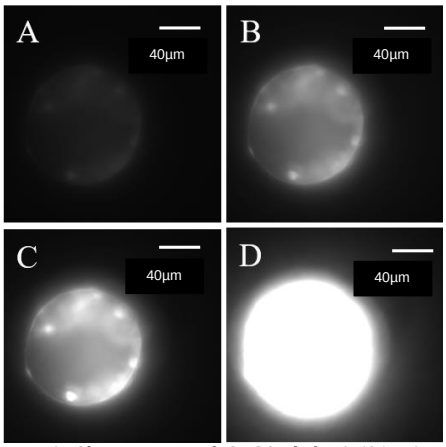

Figure 31. Low Glucose Concentration 40x Objective Lens with ORCA-Flash 4.0. (A.) 470 nm emission filter with 10% SOLA. (B.) 470 emission filter with 50% SOLA. (C.) 535 emission filter with 10% SOLA. (D.) 535 emission filter with 50% SOLA.

5.2.2 MATLAB/Image Analysis

To evaluate the image analysis algorithm the team implemented, time lapses of the CFP and YFP intensities of pancreatic islet cells exposed to varying concentrations of glucose were graphed and recorded over periods of just under 10 minutes using the Nikon TI Eclipse microscope. These treatments are summarized and displayed in Figure 32. The first treatment was a test run and the users recorded the treatment administered as a gradual transition from high glucose concentration (note that high glucose concentration refers to a concentration of 16.2 mM) to low glucose concentration (low glucose concentration refers to a concentration of 2 mM). In stark opposition to all the treatments recorded following the first treatment, the FRET

ratio increased at a steady rate despite the supposed transition from high to low glucose. It is to be noted that this treatment was likely incorrectly labeled by the researcher, however this cannot be definitively stated. Regardless, the statistical testing done on the images only compared the two imaging algorithms and not the effect of glucose on FRET ratios, so the data was still included in the analysis. The remaining treatments exhibited expected behavior. The second and third treatments represented islet cells exposed to a transition of low to high glucose concentrations, and the FRET ratios produced by these treatments agreed with the expected increase in FRET ratio over time. The final treatment administered was a transition of high to low glucose concentrations and the FRET ratios decreased over time as expected.

The data collection by the Nikon software resulted in a .csv file with the CFP and YFP intensities of each image pair collected as well as a .ncd file containing the actual image files for each picture taken by the microscope during the time lapse. Using the intensity data included in the .csv files, FRET ratios were calculated and graphed to visualize the changes in FRET ratio over time. This was repeated four times total, once for every treatment that was carried out.

To test the efficacy of the team's image analysis algorithm, the same images collected and analyzed by the Nikon software were processed using the team's software. Running the image analysis script in MATLAB, files were read in by the script and the FRET ratio for each pair of images were saved in an array. Like with the professional software data, the FRET ratios were graphed to visualize the changes in FRET ratio over time.

Now that each 'treatment' had a pair of graphs, one representing data produced from the professional software and the other representing data produced from the team's algorithm, a linear fit was applied to each graph to get a measure of the relative changes in FRET ratio over time. Using these eight slopes, two for each treatment, a paired T-test was employed to determine if these algorithms were statistically similar using the following conditions:

$$H_O: \mu_{Nikon} - \mu_{MATLAB} = 0$$
$$H_A: \mu_{Nikon} - \mu_{MATLAB} \neq 0$$

The null hypothesis represents a case in which there is no significant difference between the Nikon software and our own with the alternate hypothesis suggesting there is a significant difference between the two algorithms.

After running the paired T-Test, a P-value of 0.718 was returned, suggesting there was no significant difference between the Nikon software and our own. While this conclusion is statistically relevant, it is important to consider the context of this P-value. With P-value's closer to 1, the results would suggest a greater resemblance between the team's algorithm and the professional software. As a result, it is apparent that while the algorithm appears to function well, a more robust image analysis algorithm would produce more relevant and usable data, suggesting that future changes be made to the algorithm.

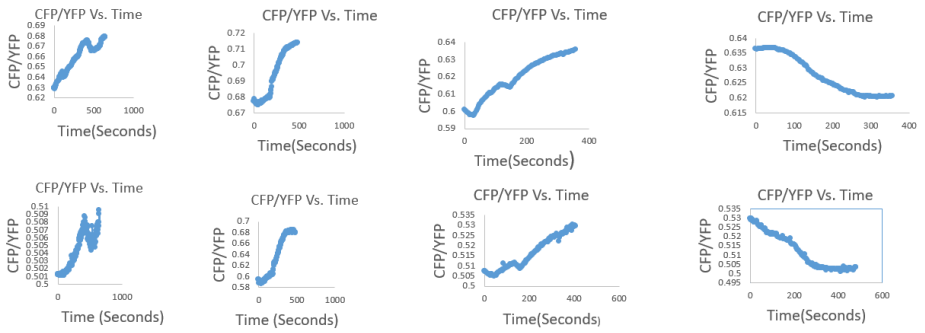

Figure 32. Top Row: FRET Ratio over time calculated by Nikon Elements. Bottom Row: FRET Ratio over time calculated with amateur software. From Left to Right: High to Low Glucose Concentration, Low to High Glucose Concentration, Low to High Glucose, High to Low Glucose. Note: CFP is equivalent to mTFP and YFP is equivalent to Venus in this specific case

5.2.3 Resolution Test Chart

Using Equation 10, the experimental spatial resolution of the microscope was calculated. The group number and element number imaged was 7 and 4, respectively, see Figure 33.

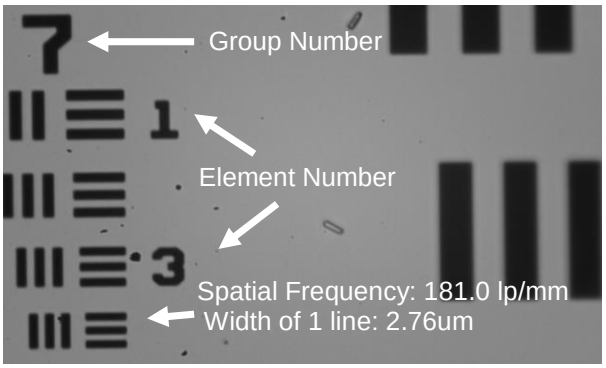

Figure 33. Image of the 1951 USAF Resolution Test Chart. The bottom row of vertical and horizontal bars under group 7 is group four.

It was determined that the spatial resolution was 5.5 µm by using Equation 12.

$$Resolution\ (\mu m) = \frac{1000}{2^{Group+(element-1)/6}} \qquad (12)$$

$$5.5\ \mu m = \frac{1000}{2^{7+(4-1)/6}} \qquad (12.1)$$

Using Equation 5, the diffraction limited resolution is calculated to about 0.5 µm. The difference between the experimental and the diffraction-limited resolution makes sense because Equation 5 only accounts for the numerical aperture and does not account for the detector or the choice in tube lens. As previously mentioned in section 3, the tube lens required for an optimal spatial resolution with the given camera is 150mm. Additionally, the team did not have a sensitive enough focuser to move the resolution test chart such that higher element numbers could be imagined. In the future, the resolution test chart could be imagined with a more sensitive focuser such that smaller bars on the chart could be imagined; furthermore, the objective to be used in the final design should be used to image the chart.

6. Future Work

The next steps for the team will be to purchase the remaining parts needed to assemble the microscope. This includes the posts, as well as a more permanent solution to the final assembly of the microscope. Specifically, the team must ensure that the light source is properly mounted and attached securely to the heat sink. This will ensure that the microscope does not shift during transport and is supported during use. The team will likely need to purchase a base plate to hold these items, but they will still need to be fastened to the plate. The team will also look to enclose some parts of the microscope, especially those that would be sensitive to spills, such as open electronics.

There are several design changes to the software and circuitry that would improve the functionality and user experience of the microscope. Although the current GUI is functional, the user interface of the design is very basic and unintuitive. Improvements will be made to the overall design of the user interface to make the software a more complete and desirable package. Additionally, the current image processing algorithm gives a good estimate of the FRET ratio between donor and acceptor images; however the absence of image processing techniques used to eliminate potential crosstalk between the donor and acceptor leads to a less accurate estimation of FRET ratio. Implementing some basic image processing techniques to account for this issue will improve the reliability of our system. The team would also like to explore options that make adjusting the light source more user friendly. Currently, the circuit contains a potentiometer that is adjusted without knowing the effects on the light source. Analysis should be done to evaluate the range of currents that the adjusting potentiometer creates and further, the amount of light that results from the LEDs. Implementing some sort of external case to the circuit with a handle that provides known thresholds could be a solution to this problem. The group also would like to move the current circuits used to control the light source and the filter swapper over to a PCB board to improve the ergonomics and user-friendliness of the device.

Additionally, the microscope is supposed to be a prototype, and ideally the team will be able to decrease the overall cost of each individual microscope by replacing parts with 3D printing or machined parts. To do this, the team will complete a cost analysis where we will determine the most expensive pieces of the current set-up as well as how much money could be saved by replacing each of these parts with a custom part instead. The initial budget of $2,000 would be the goal for each prototype, but this will depend on the cost of the main components;

the camera and objective. One item that the team could replace is the z-adjustment knob that we purchased, which could be replaced with a rack and pinion made of a combination of a purchased metal rack and pinion with a 3D-printed piece.

After the initial prototype is complete, the team plans to run a time lapse experiment in Professor Merrins's Lab. The team will compare the data acquired with his microscope to that acquired with from the prototype microscope. However, we will need to consider how the experiments will be performed since we cannot ensure that we will be imaging the same cells. The cells would need to be transferred between the microscopes or two separate islets would need to be used independently. Therefore, we would need to include some sort of control or normalization and then we could analyze the data using a paired t-test on the calculated FRET ratios. After this, the team would like to use the yeast that Professor Merrins plans to use in his lab to run the test exactly as students would in the lab.

Following testing, if the system does not provide the results we expect, we will need to modify specific components. If the problem is with the images or FRET analysis we could use a different camera, vary the optics, use a different light source, or alter our code for FRET analysis. Altering the code is likely the cheapest change to make, and we can look at making it more like commercial versions. Next we could see if the optics are the problem by comparing a time lapse with our camera on Professor Merrins' set-up to a time lapse with our camera on our microscope. If the time lapse analysis is significantly better on his set-up, it is likely that our light source or other optics are the reason for the poor FRET results. We could use different tube and objective lens combinations depending on if our images have too small of a field of view or are not bright enough. Finally, we may need to consider buying a camera with a higher dynamic range or higher quantum efficiency which would mean additional cost to our design. However, between a cheaper dysfunctional microscope and a slightly more expensive working version, the client would prefer the latter.

Following development of the working prototype, the team will compile the work of the semester into a comprehensive summary. Since the client wants to be able to assemble more of these himself, the team will need to provide a guide. First, the guide will need to include a bill of materials as well as the SolidWorks files that he will need to print. We will likely want to reduce the number of parts he will need to machine, but if there are some, they should be relatively simple to machine, and we could provide contact information for him so that he could also hire somebody to do the machining for him. Finally, we will need to provide an instruction manual for the assembly of the microscope so that he can build the future ones himself. With this manual completed, the team could potentially approach WARF once more to determine if the final product could be patented. However, at the very least, the team would like to publish a paper with an open source journal and/or website so that other labs throughout the country could make their own microscopes.

7. Conclusion

This semester the team spent time designing and building a microscope for fluorescence resonance energy transfer imaging. Unlike traditional FRET microscopes, this device is for a specific function: a few assays utilizing the client's Laconic FRET-based biosensor. The goal of this project is to build a single prototype that his students would be able to use in his biochemistry class. One of the experiments they will perform is to study how changing the

glucose concentration in time changes the FRET ratio. Once complete, the miniature microscope should have features like those of his lab's current microscope and, among other components, it must include an excitation source, a camera, and a series of filters all for under a budget of $4,000. After further research and various meetings with the team's client and advisor, the team decided to first build the microscope out of Thorlabs components.

Currently, the team has built a microscope with our own components besides additional optical posts and the objective lens, which should be swapped out with the one the client is providing. The camera has been tested against the client's camera, and our software has been tested against the client's software (Nikon Elements). The software was initially developed in MATLAB, but since the filter swap and camera are being controlled with Microsoft Visual Studios, the team transferred the image analysis code into this programming language as well. The light source was designed to provide the excitation wavelength to the sample through a series of a dichroic mirror and an excitation filter. Once the excitation occurs, the camera will acquire images at both 535 and 470 nm using the Thorlabs filter swap.

Now that the prototype is mostly complete, the team can begin to test its functionality and attempt to narrow down which parts of the prototype are essential and which need to be improved. Through well-designed tests we can improve the microscope as well as decrease its cost, which will be the focus of the next semester. By the end of the school year, the team will have finalized and optimized the design and protocol so that students in Professor Merrins' lab are able to operate it and run through the desired protocol. Ideally, we will have also completed the accompanying instruction manual so that we can either attempt to patent our design or publish a paper to disseminate the information for teaching labs across the country.

8. Acknowledgements

The team would like to thank their advisor Professor Jeremy Rogers and their client Professor Matthew Merrins for guiding them through the design process. In addition, special thanks also goes out the entire BME department for providing helpful resources for this design project.

9. References

[1] A. San Martin, S. Ceballo, I. Ruminot, R. Lerchundi, W. Frommer and e. al, "A Genetically Encoded FRET Lactate Sensor," *PLOS ONE,* 2013.

[2] "Fluorescence Resonance Energy Transfer," Chemistry LibreTexts, 2017. [Online]. Available: https://chem.libretexts.org. [Accessed 26 April 2017].

[3] R. Clegg, "Chapter 1: Förster Resonance Energy Transfer-FRET," Science Direct, 2017. [Online]. Available: http://www.sciencedirect.com. [Accessed 26 April 2017].

[4] "Blood Test: Lactate Dehydrogenase (LDH)," Kidshealth.org, 2017. [Online]. Available: http://kidshealth.org. [Accessed 18 February 2017].

[5] "LD," Lab Tests Online, 2017. [Online]. Available: https://labtestsonline.org. [Accessed 18 February 2017].

[6] R. N. Day, C. F. Booker and A. Periasamy, "Characterization of an improved donor fluorescent protein for Förster resonance energy transfer microscopy," *Journal of Biomedical Optics,* vol. 13, no. 3, p. 31203, 2008.

[7] T. Nagai, K. Ibata, E. S. Park, M. Kubota, K. Mikoshiba and A. Miyawaki, "A variant of yellow fluorescent protein with fast and efficient maturation for cell-biological applications," *Nature Biotechnology,* vol. 20, no. 1, pp. 87-90, 2002.

[8] P. Kuchel, B. Chapman, A. Lovric, J. Raftos, M. Stewart and D. Thorburn, "The relationship between glucose concetration and rate of lactate production by human erythrocytes in an open perfusion system," *Elsevier,* vol. 805, pp. 191-203, 1984.

[9] "Dino-Lite Digital Microscope," Dino-Lite, 2017. [Online]. Available: http://www.dino-lite.com. [Accessed 16 February 2017].

[10] "Lumascope 620," Etaluma, 2017. [Online]. Available: http://www.etaluma.com. [Accessed 16 February 2017].

[11] "Stereo Microscope Fluorescence Adapter," Nightsea, 2017. [Online]. Available: http://www.nightsea.com. [Accessed 16 February 2017].

[12] C. Stewart and J. Giannini, "Inexpensive, Open Source Epifluorescence Microcopes," *Journal of Chemical Education,* vol. 93, pp. 1310-1315, 2016.

[13] "Eclipse Ti-E Inverted Microscope System," Nikon, 2017. [Online]. Available: https://www.nikoninstruments.com. [Accessed 09 October 2017].

[14] "Infinity Corrected Optics," Microscope World, 2017. [Online]. Available: https://www.microscopeworld.com/t-infinity_corrected_optics.aspx. [Accessed 8 December 2017].

[15] M. Abramowitz and M. W. Davidson, "Numerical Aperture and Resolution," Molecular Expressions, 13 November 2015. [Online]. Available: https://micro.magnet.fsu.edu/primer/anatomy/numaperture.html. [Accessed 8 December 2017].

[16] K. R. Spring, N. S. Claxton and M. W. Davidson, "Nikon CFI60 Optical System,"

MicroscopyU, 2017. [Online]. Available: https://www.microscopyu.com/microscopy-basics/nikon-cfi60-optical-system. [Accessed 8 December 2017].

[17] M. W. Davidson, "Introduction to Microscope Objectives," Microscopy U, 2017. [Online]. Available: https://www.microscopyu.com/microscopy-basics/introduction-to-microscope-objectives. [Accessed 8 December 2017].

[18] S. T. A. H. H. G. Timo Gissibl, "Two-photon direct laser writing of ultracompact mult-lens objectives," *nature photonics,* vol. 10, pp. 554-560, 2016.

[19] J. G. Webster, Bioinstrumentation, Hoboken: John Wiley & Sons, Inc., 2004.

[20] "Microscope Objective, Tube, and Scan Lens Tutorials," Thorlabs, 2017. [Online]. Available: https://www.thorlabs.de/newgrouppage9.cfm?objectgroup_id=10764. [Accessed 8 December 2017].

[21] J. Jo, M. Y. Choi and D.-S. Koh, "Size Distribution of Mouse Langerhans Islets," *Biophysical Journal,* vol. 93, pp. 2655-2666, 2007.

[22] "Chroma Inc.," 2017. [Online]. Available: https://www.chroma.com/products/sets/89006-et-ecfp-eyfp-mcherry.

[23] "Vollong 3W White High Power LEDs," Super Bright LEDs Inc., 2017. [Online]. Available: https://www.superbrightleds.com. [Accessed 09 October 2017].

[24] P. Horowitz, The Art of Electronics, vol. 2, Cambridge University Press, 1989.

[25] "Lambda TLED/TLED+," Sutter Intrument, 2012. [Online]. Available: https://www.sutter.com. [Accessed 9 October 2017].

[26] "SOLA light engine," Lumencor Inc., 2017. [Online]. Available: http://www.lumencor.com. [Accessed 9 October 2017].

[27] "mTFP1," Allelebiotech.com, 2017. [Online]. Available: http://www.allelebiotech.com. [Accessed 12 April 2017].

[28] P. Sarkar, S. Kouschik, S. Vogel, I. Gryczynski and Z. Gryczynski, "Photophysical Properties of Cerulean and Venus Fluorescent Proteins," *Journal of Biomedical Optics,* 2009.

[29] P. Kuchel, B. Chapman, A. Lovric, J. Raftos, M. Stewart and D. Thurman, "The relationship between glucose concentration and rate of lactate production by human erythrocytes in an open perfusion system," *Elsevier,* vol. 805, pp. 191-203, 1984.

10. Appendices

Appendix A.

Product Design Specifications
Miniature Fluorescent Microscope

Team Members: Ben Ratliff, Ethan Nethery, Kaitlyn Gabardi, John Rupel, Kadina Johnston
BME 400
Client: Professor Matthew Merrins
Advisor: Professor Jeremy Rogers
Last Updated: December 12th, 2017

Problem Statement: The client, Professor Matthew Merrins, teaches human biochemistry lab at the University of Wisconsin-Madison. The course focuses on the enzyme lactate dehydrogenase, which produces lactate from pyruvate. Currently, his lab utilizes Laconic, a Förster Resonance Energy Transfer (FRET)-based biosensor. This biosensor detects the presence of Lactate in healthy, living cells, but the fluorescence must be monitored in time lapse using a high cost microscope. This microscope excites the lactate biosensor using a system of high power LEDs and a filter wheel, and the fluorescence is recorded. The project goal to to build a lower-cost, limited alternative to the client's more expensive microscope

Function: The final design will be a single prototype device that will allow his students to measure FRET in his human biochemistry class. This device will be similar to his lab's microscope as it will contain an excitation source, two different filters for FRET, and a camera that will capture the images of the specimen in the solution chamber.

Client Requirements:

- Initial prototype built must be made under $4,000
    - Eventually build multiple devices around $2,000
- Compact and intuitive for student use
- Software used to process images must be free
- Easy to obtain FRET results
- Device should be able to detect yeast cells
- Result should be similar to results obtained from client's microscope

- Should be an inverted design
- Interchangeable filters and excitation source
- Device can be repeatedly manufactured with limited engineering experience required
- Microscope should have significant and detectable change in fluorescence upon stimulation between 470 and 535 nm from 430 nm excitation source

Physical and Operational Characteristics:

A. *Performance Requirements:* The designs must be able to accurately measure light intensities at 470 and 535 nm. These readings do not have to be simultaneous, but must be close in time. An excitation source of 430 nm should induce this response, which will be recorded by a detector (camera) and uploaded to a freeware image analysis program (ImageJ) on a compatible computer for analysis. The lactate level can then be extracted based on the ratio of 470 and 535 intensities.

B. *Safety:* The design should minimize contact between the excitation source and user. This is due to the fact that the excitation source is near the UV light spectrum which is damaging to human skin tissue. All electronic components should be enclosed.

C. *Accuracy and Reliability:* This product should be accurate enough to determine the acceptor-donor ratio. FRET results should be similar to the results obtained from the client's microscope.

D. *Life in Service:* Product itself would last for years and system components should be easily replaced if broken or damaged.

E. *Shelf Life:* Shelf life would be 50 years. Optical filters and CMOS cameras will have lifetime guarantee as long as proper care is given to these components.

F. *Operating Environment:* The design must operate at room temperature.

G. *Ergonomics:* Product should be simple and intuitive for students to use. The image collection and accept/donor ratio calculation should be as simple as possible.

H. *Size:* Able to be used as a typical laboratory station on a lab desk (8" x 14" base), size similar to competing/conventional microscopes. All non-essential components for analysis should be discarded. Height of microscope < 45 cm.

I. *Power Source:* Device will be powered by a power outlet from the wall, thus eliminating the need for battery replacement.

J. *Weight:* 1 to 10 pounds

K. *Materials:* The device will have an internal circuit and will utilize a single, super-bright white LED, plastics, wires, optical filters, and an Arduino. A CMOS camera will be used along with a stepper motor for the mobile filter swap. Two emission filters and one excitation filter will be used in order to differentiate the 470 nm and 535 nm fluorescence. The final product will also include 3D printed parts such as the LED holder, filter swap platform and stand, which will be fabricated out of PLA and ABS.

L. *Aesthetics, Appearance, and Finish:* Simple aesthetics, appears intuitive to use, and simple finish.

Production Characteristics:

A. *Quantity*: One prototype with ability to be repeatedly fabricated over time with plans to have a total of six to eight devices would be implemented over an 8 semester period.
B. *Target Product Cost:* Max cost is $4,000.
    a. Goal is to make final product around $2,000

Miscellaneous:

A. *Standards and Specifications*: Should comply with current FRET analysis protocol and/or be adapted into a simple protocol for the client's human biochemistry class teaching lab analysis.
B. *Patient-Related Concerns*: Cost is the highest determinant in design. The functionality should be sufficient for teaching purposes on a budget of 1/30 of current device. A typical Nikon microscope can cost between $50,000 and $120,000, and the client would like the device to be between $2,000 and $4,000. Resolution is not a key concern, only that the difference in emission intensities can be accurately extracted from experimentation. The data collection is the largest concern, and data analysis should be used by an easily accessible freeware service.

C. *Competition*:

a. Dino-Lite:
    i. This product is small fluorescence microscope where each type of microscope has a specific wavelength and filter designed for specific fluorophores. They are not ideal for FRET since fret requires the use of two fluorophores.
b. Lumascope 620:
    i. This product is for professional use. It can be used for a variety of fluorescence microscopy techniques. It is expensive due to its broad capabilities
c. 3D Printed OPN Scope
    i. This device uses 3D printing to make the outer shell, drawer for the fluorescence filter tude, and tube that holds the eyepiece and light source. A 3D printed device

allows the capability to modify the structural parts of the microscope, in addition to making the device extremely cheap to fabricate as compared to customized part manufactured from different companies.

d. Nighsea:
    i. This product converts a Stereo microscope into a simple fluorescence microscope. Using an attachable filter and an external light source the microscope can detect light from fluorophores. The lens are designed for specific fluorophores and is not ideal for FRET.

D. *Customer:* Human biochemistry lab (BMC 504) instructor and students. Future potential for other teaching labs to incorporate our design but their own sets of filters.

Appendix B.

Single-Shot Design Schematic. This is the first design idea proposed and it consists of no moving parts.

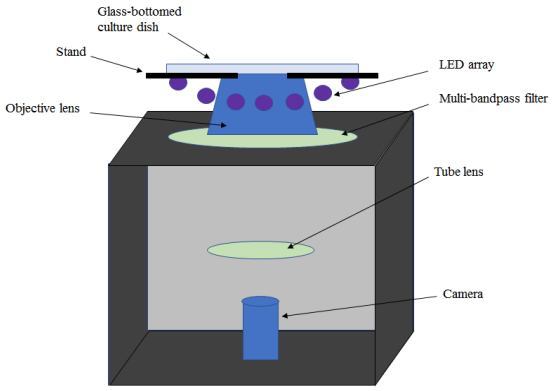

Filter-Swap Design Schematic. This is the second design idea proposed and it consists of a motor that swaps out the filters.

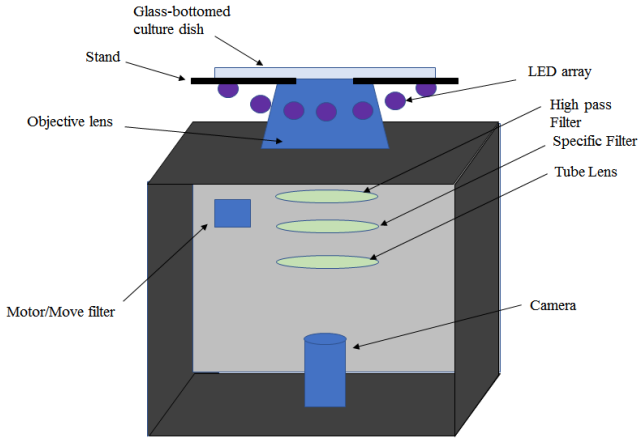

Beam-Splitter Design Schematic. This is the third proposed design and it consists of mirror that splits the two wavelengths of interest.

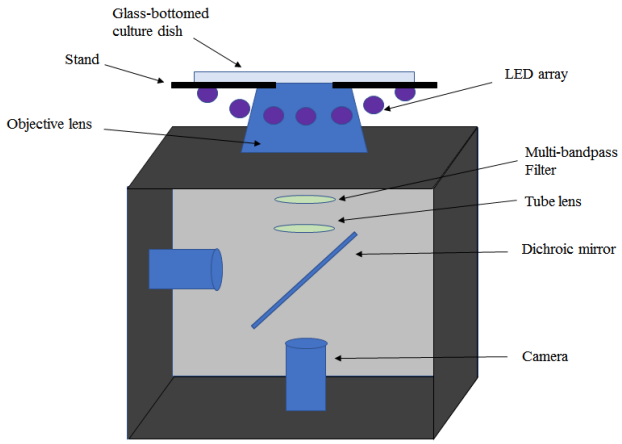

Appendix C.

Circuit to power LED array from previous Spring 2017.

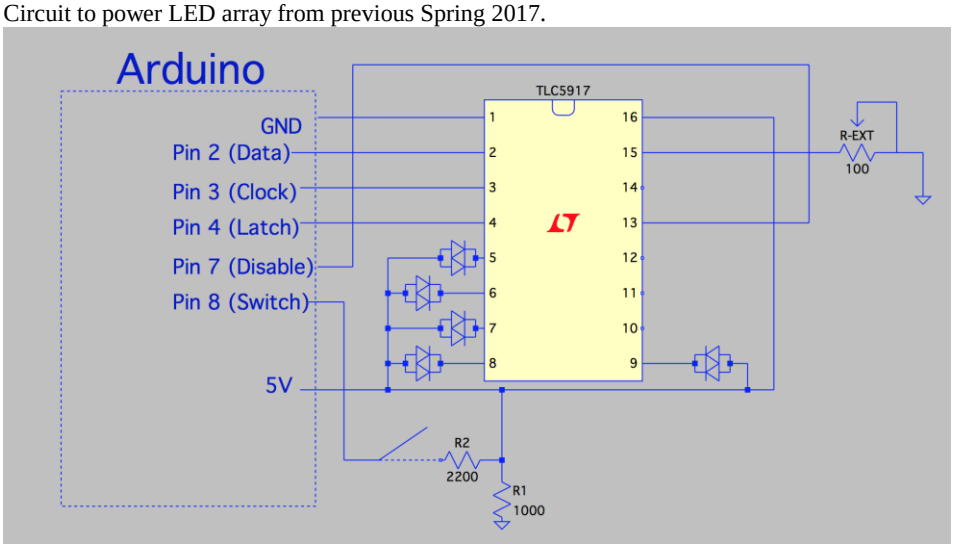

Appendix D.

The Imaging Source DMK42BUC03 Specifications

Sensor Type: CMOS

Sensor Model: Micron* MT9M021

Shutter: Global

Pixel Size: 3.75um X 3.75um

Sensor Size: 4.8mm X 3.6mm

Signal to Noise Ratio: 38dB

Dynamic Range: 8 bit

Frame Rate:

Quantum Efficiency: Above 64% between 450nm and 600nm

*Micron was acquired by ON Semiconductor

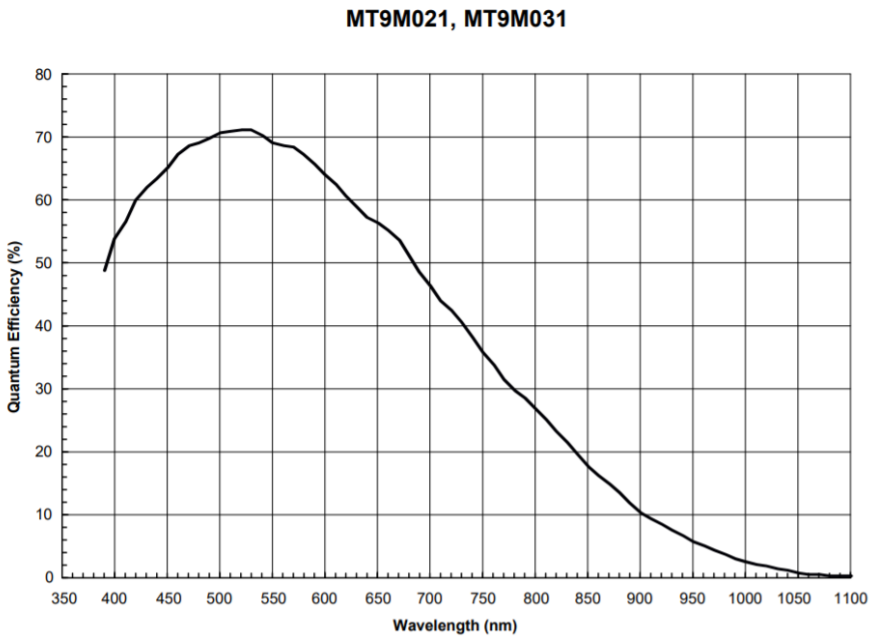

Appendix E.

Glossary of terms that are used to describe optical sensors

CMOS: Complementary metal oxide semiconductor, is a type of otpical sensor. Typically cheaper than CCD sensors. Light is directly converted to electricity in every pixel

CCD: charged coupled devices, another type of optical sensor, Typically more expensive, but takes better quality images than CMOS sensors. CCD outputs the charge of each pixel, (charge is not the same as voltage), to a limited number of nodes and then the charge is converted to a voltage.

Shutter: A shutter determines how the pixels are activated. In a rolling shutter, a row of pixels is read out and then the next row and so on and so forth until the last row. A global shutter reads all the pixel values at once.

Pixel: The pixels are the elements that make up an image sensor. The pixel collects the charge of the light.

Signal to Noise Ratio: A ratio of the signal of interest to the noise of the camera. A large signal to noise ratio indicates the sensor has low noise. Usually measured in decibels. Accounts for both shot noise and temporal dark noise

Dynamic Range(definition one): The ability of the sensor to detect the difference in light intensity when the light intensity is very similar.

Dynamic Range(definition two): Ratio of signal to noise, but only accounting for temporal dark noise.

Quantum Efficiency: The percentage of photons converted to an electrical signal

Temporal Dark Noise(aka read noise): The amount of error associated with a signal

Shot Noise: The square root of the signal. Shot noise is the amount of noise in the light source itself.

Absolute Sensitivity Threshold: The number of photons needed to create a signal equivalent to the noise of the camera.

Saturation Capacity(aka Well Depth): The amount of electrons that can be stored in a pixel

Frame Rate: A measure of how fast a sensor can acquire and output an image. Measured in Hertz(Hz) or Frames per second (fps).

Appendix F.

Specifications of Prof. Merrin's Nikon Objective

Numerical Aperture: 0.75
Working Distance: 1mm
Magnification: 20x
Type: Super Flour
Mounting Threads: M25 X 0.75
Designed for 200mm tube lens

Appendix G.

Glossary of terms used to describe optical objective

Numerical Aperture: Ability of microscope to collect light and resolve details. Unitless higher is better

Working Distance: Distance from the outer objective lens to the specimen's cover slip.

Achromatic: Most affordable objective, corrected for two wavelengths, Significant Abbreviations when using green light

Fluorite: Have higher Numerical Apertures then achromatic objectives. Made with special minerals to reduce auto fluorescence. Corrected spherically for two or three wavelengths of light. Corrected chromatically for two or three colors
Apochromatic: Most expensive and optically corrected objective type. Complicated lens system
PLAN: Simply means the objective corrects for curvatures in the image

Appendix H.
Comparison of quantum efficiencies of cameras
On the left is the imaging source QE graph and the right is the Orca Flash 4.0 QE graph. Obviously the Orca has a higher QE.

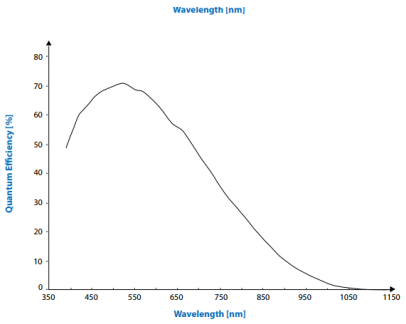

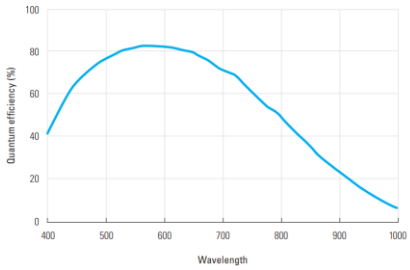

Appendix I.
Code for Arduino:

```
#define fwdPin      7
#define bkdPin      6
#define inMotionPin  4
#define fwdLedPin   11
#define bkdLedPin   12
#define pwrPin      8
#define transistorPin 2
#define pwrLedPin   10
#define BaudRate 9600
char incomingOption;

void setup()
```

```
{
  digitalWrite(pwrPin, HIGH);
  digitalWrite(fwdPin, HIGH);
  digitalWrite(bkdPin, HIGH);
  // initialize the fwdPin as an output:
  pinMode(fwdPin, OUTPUT);
  // initialize the fwdPin as an output:
  pinMode(bkdPin, OUTPUT);
  // initialize the fwdPin as an output:
  pinMode(inMotionPin, INPUT);
  pinMode(fwdLedPin, OUTPUT);
  pinMode(bkdLedPin, OUTPUT);
  pinMode(pwrLedPin, OUTPUT);
  pinMode(pwrPin, OUTPUT);
  pinMode(transistorPin, OUTPUT);
  Serial.begin(BaudRate);
}
void loop()
{
   incomingOption = Serial.read();
   switch(incomingOption){

     case '0':
       digitalWrite(fwdPin, LOW);
       digitalWrite(fwdLedPin, HIGH);
       digitalWrite(fwdPin, HIGH);
       delay(2000);
       Break;
     case '1':
       digitalWrite(bkdPin, LOW);
       digitalWrite(bkdLedPin, HIGH);
       digitalWrite(bkdPin, HIGH);
       delay(2000);
       break;
     case '2':
       digitalWrite(pwrPin, LOW);
       digitalWrite(pwrLedPin, HIGH);
```

```
        break;
      case '3':
        //Turn ON LED
        digitalWrite(transistorPin, HIGH);
        break;
      case '4':
        //Turn OFF LED
        digitalWrite(transistorPin, LOW);
        break;
    }
}
```

Appendix J.
Code for GUI in Visual Studios

```
using System;
using System.Collections.Generic;
using System.ComponentModel;
using System.Data;
using System.Drawing;
using System.Linq;
using System.Text;
using System.Threading.Tasks;
using System.Windows.Forms;
using Emgu.CV;
using Emgu.Util;
using Emgu.CV.Structure;


namespace MicroGUI
{
   public partial class Form1 : Form
   {
      // I may just return the values of the fretRatioTL in the time lapse method and set the int array of timeCord to 0 through 119
      // private int[] timeCord;
      // private float[] fretRatioTL;

      public Form1()
      {
```

```
    InitializeComponent();
    this.Load += Form1_Load;
}

private void Form1_Load(object sender, System.EventArgs e)
{
    //Load possible com Ports into the combo box
    var ports = System.IO.Ports.SerialPort.GetPortNames();
    comboBox1.DataSource = ports;
}

private void cmdStartLive_Click(object sender, EventArgs e)
{
    icImagingControl1.LiveStart();
}

private void cmdStopLive_Click(object sender, EventArgs e)
{
    if (icImagingControl1.LiveVideoRunning == true)
    {
        icImagingControl1.LiveStop();
    }
}

private void cmdSaveBitmap_Click(object sender, EventArgs e)
{
    SaveFileDialog saveFileDialog1;
    icImagingControl1.MemorySnapImage();
    saveFileDialog1 = new SaveFileDialog();
    saveFileDialog1.Filter = "bmp files (*.png)|*.png|All files (*.*)|*.*";
    saveFileDialog1.FilterIndex = 1;
    saveFileDialog1.RestoreDirectory = true;

    if (saveFileDialog1.ShowDialog() == DialogResult.OK)
    {
        icImagingControl1.MemorySaveImage(saveFileDialog1.FileName);
    }
}

//CONNECT BUTTON
```

```
private void button1_Click(object sender, EventArgs e)
{
   try
   {
      port.Open();
   }
   catch (Exception ex)
   {
      port.Close();
      port.Dispose();
   }
}

private void Connect(string portName)
{
   port.PortName = portName;

   if (!port.IsOpen)
   {
      port.DataBits = 8;
      port.StopBits = System.IO.Ports.StopBits.One;
      port.BaudRate = 9600;
   }
}

//SELECT BUTTON
private void button2_Click(object sender, EventArgs e)
{
   port.Write("2");
   System.Threading.Thread.Sleep(5000);
   port.Write("*");

   port.Write("1");
   System.Threading.Thread.Sleep(5000);
   port.Write("*");

   port.Write("0");
   System.Threading.Thread.Sleep(5000);
   port.Write("*");
```

```
    textBox1.Text = "470nm Filter in Place";


    //Disable Forwardbutton
    button3.Enabled = false;
    //Enable Backwardbutton
    button4.Enabled = true;

}

//FORWARD BUTTON
private void button3_Click(object sender, EventArgs e)
{
    port.Write("*");
    port.Write("0");
    System.Threading.Thread.Sleep(500);

    textBox1.Text = "470nm Filter In Place";

    //Disable Forwardbutton
    button3.Enabled = false;
    //Enable Backwardbutton
    button4.Enabled = true;
}

//BACKWARD BUTTON
private void button4_Click(object sender, EventArgs e)
{
    port.Write("*");
    port.Write("1");
    System.Threading.Thread.Sleep(500);

    textBox1.Text = "535nm Filter In Place";

    button4.Enabled = false;
    button3.Enabled = true;
}

private void comboBox1_SelectedIndexChanged_1(object sender, EventArgs e)
{
```

```
            if (comboBox1.SelectedIndex > -1)
            {
                Connect(comboBox1.SelectedItem.ToString());
            }
            else
            {
                MessageBox.Show("Please select a port first");
            }
        }

        //ON Button
        private void button5_Click(object sender, EventArgs e)
        {
            port.Write("3");
        }

        //OFF Button
        private void button6_Click(object sender, EventArgs e)
        {
            port.Write("4");
        }

        // FRET Button
        private void button7_Click(object sender, EventArgs e)
        {
            ImageProcess("E:\\BME 400\\Low Glucose(2mmol)\\Imaging
Source\\TIS_LG_430ex_470em.tif", "E:\\BME 400\\Low Glucose(2mmol)\\Imaging
Source\\TIS_LG_430ex_535ex.tif");
        }

        private void button8_Click(object sender, EventArgs e)
        {
            TimeLapse();
        }


        private void Form1_Load_1(object sender, EventArgs e)
        {
        }
```

```
// Make a button that when you click it runs a function

// This function will essentially calulate the FRET ratio for images and then records the ratio and time in two arrays
// Then finish the function by graphing the arrays

// Also make a button that carries out a function that calculates the FRET ratio at a single picture?

// Mat cfp_LG_Filename = CvInvoke.Imread("E:\\BME 400\\Low Glucose(2mmol)\\Imaging Source\\TIS_LG_430ex_470em.tif", Emgu.CV.CvEnum.ImreadModes.AnyColor);

private void TimeLapse()
{
   button5_Click(new object(), new EventArgs());

   int[] timeCord = new int[120];
   float[] fretRatioTL = new float[120];
   //Array.Clear(GetTimeCord(), 0, GetTimeCord().Length);
   //Array.Clear(GetFretRatioTL(), 0, GetFretRatioTL().Length);

   for (int i = 0; i < 120; i++)
   {
      takePic(i, "CFP");
      System.Threading.Thread.Sleep(1000);

      // this mayyyyy not work, if not just implement the code from this method orrrrr a better option may be to rewrite the same method except without a button click

      button4_Click(new object(), new EventArgs());
      System.Threading.Thread.Sleep(1000);

      takePic(i, "YFP");

      button3_Click(new object(), new EventArgs());

      //SetTimeCord(i, i);
      timeCord[i]=i;
      float tempFret;
```

```
            tempFret = ImageProcess("C:\\Users\\Ethan Nethery\\Desktop\\BME
400\\Timelapse\\picCFP" + i.ToString() + ".jpeg", "C:\\Users\\Ethan Nethery\\Desktop\\BME
400\\Timelapse\\picYFP" + i.ToString() + ".jpeg");

            fretRatioTL[i] = tempFret;
            //SetFretRatioTL(i, tempFret);

        }

    }

    private void takePic(int picNum, String filter)
    {
        icImagingControl1.LiveStop();
        icImagingControl1.MemorySnapImage();
        icImagingControl1.MemorySaveImage("C:\\Users\\Ethan Nethery\\Desktop\\BME
400\\Timelapse\\pic" + filter + picNum.ToString() + ".jpeg");
        icImagingControl1.LiveStart();
    }
    private float ImageProcess(String cfpFilePath, String yfpFilePath)
        {

            // "E:\\BME 400\\Low Glucose(2mmol)\\Imaging Source\\TIS_LG_430ex_470em.tif"

            Image<Gray, float> cfp_LG = new Image<Gray, float>(cfpFilePath);
            Image<Gray, float> cfpMedian = cfp_LG.SmoothBlur(5, 5);
            Bitmap usableCFPMedian = cfpMedian.ToBitmap();

        // "E:\\BME 400\\Low Glucose(2mmol)\\Imaging Source\\TIS_LG_430ex_535ex.tif"

            Image<Gray, float> yfp_LG = new Image<Gray, float>(yfpFilePath);
            Image<Gray, float> yfpMedian = yfp_LG.SmoothBlur(5, 5);
            Bitmap usableYFPMedian = yfpMedian.ToBitmap();

            // pictureBox1.Image = usableCFPMedian;

            Image<Gray, float> diff = yfpMedian - cfpMedian;

            //Image<Gray, float> tempCFP = new Image<Gray, float>(1280, 960);
            //Image<Gray, float> tempYFP = new Image<Gray, float>(1280, 960);
```

```
            //int row = 960;
            //int column = 1280;
            int z = 0;

            Image<Gray, float> ratio = new Image<Gray, float>(1280, 960);
            Image<Gray, float> binRat = new Image<Gray, float>(1280, 960);

            for (int i = 0; i < 960; i++)
            {
               for (int j = 0; j < 1280; j++)
               {
               // i think for a bgr image, data's third parameter is an array from 0 to 2 representing the intensity of blue, green and red
               // this would suggest that for a gray image, only parameter 0 is true

               // && diff.Data[i, j, 0] >= -30
               if (Math.Abs(diff.Data[i, j, 0]) <= 30 )
                  {
                     ratio.Data[i, j, 0] = 0;
                     binRat.Data[i, j, 0] = 0;
                  }
                  else
                  {
                     ratio.Data[i, j, 0] = Math.Abs(cfpMedian.Data[i, j, 0]) / Math.Abs(yfpMedian.Data[i, j, 0]);
                     binRat.Data[i, j, 0] = 255;
                     z = z + 1;
                  }
               }
            }

         float[] values = new float[z];
         int hold = 0;

            for (int i = 0; i < 960; i++)
            {
               for (int j = 0; j < 1280; j++)
               {
                  if (binRat.Data[i, j, 0] == 0)
                  {
```

```
                continue;
            }
            else
            {
                values[hold] = ratio.Data[i, j, 0];
                hold = hold + 1;
            }
        }
    }

    float finalRatio;
    if (values.Length != 0)
    {
        finalRatio = values.Average();
        textBox2.Text = finalRatio.ToString();
    }
    else
    {
        finalRatio = 0;
        textBox2.Text = finalRatio.ToString();
    }

    return finalRatio;
    }

  private void textBox3_TextChanged(object sender, EventArgs e)
  {

  }

  private void textBox5_TextChanged(object sender, EventArgs e)
  {

  }
}
}
```

Appendix K.

```
using System;
using System.Collections.Generic;
```

```
using System.ComponentModel;
using System.Data;
using System.Drawing;
using System.IO.Ports;
using System.Linq;
using System.Text;
using System.Threading.Tasks;
using System.Windows.Forms;

namespace MicroGUI
{
   partial class Form1
   {
      /// <summary>
      /// Required designer variable.
      /// </summary>
      private System.ComponentModel.IContainer components = null;

      /// <summary>
      /// Clean up any resources being used.
      /// </summary>
      /// <param name="disposing">true if managed resources should be disposed; otherwise, false.</param>
      protected override void Dispose(bool disposing)
      {
         if (disposing && (components != null))
         {
            components.Dispose();
         }
         base.Dispose(disposing);
      }

      #region Windows Form Designer generated code

      /// <summary>
      /// Required method for Designer support - do not modify
      /// the contents of this method with the code editor.
      /// </summary>
      private void InitializeComponent()
      {
```

```
        this.components = new System.ComponentModel.Container();
        System.ComponentModel.ComponentResourceManager resources = new
System.ComponentModel.ComponentResourceManager(typeof(Form1));
        this.icImagingControl1 = new TIS.Imaging.ICImagingControl();
        this.cmdStartLive = new System.Windows.Forms.Button();
        this.cmdStopLive = new System.Windows.Forms.Button();
        this.cmdSaveBitmap = new System.Windows.Forms.Button();
        this.comboBox1 = new System.Windows.Forms.ComboBox();
        this.button1 = new System.Windows.Forms.Button();
        this.button2 = new System.Windows.Forms.Button();
        this.button3 = new System.Windows.Forms.Button();
        this.button4 = new System.Windows.Forms.Button();
        this.textBox1 = new System.Windows.Forms.TextBox();
        this.button5 = new System.Windows.Forms.Button();
        this.button6 = new System.Windows.Forms.Button();
        this.port = new System.IO.Ports.SerialPort(this.components);
        this.textBox2 = new System.Windows.Forms.TextBox();
        this.button7 = new System.Windows.Forms.Button();
        this.button8 = new System.Windows.Forms.Button();
        this.textBox3 = new System.Windows.Forms.TextBox();
        this.textBox4 = new System.Windows.Forms.TextBox();
        this.textBox5 = new System.Windows.Forms.TextBox();
        this.textBox6 = new System.Windows.Forms.TextBox();
        this.textBox7 = new System.Windows.Forms.TextBox();
        ((System.ComponentModel.ISupportInitialize)(this.icImagingControl1)).BeginInit();
        this.SuspendLayout();
        //
        // icImagingControl1
        //
        this.icImagingControl1.BackColor = System.Drawing.Color.White;
        this.icImagingControl1.DeviceListChangedExecutionMode                    =
TIS.Imaging.EventExecutionMode.Invoke;
        this.icImagingControl1.DeviceLostExecutionMode                           =
TIS.Imaging.EventExecutionMode.AsyncInvoke;
        this.icImagingControl1.DeviceState                                       =
resources.GetString("icImagingControl1.DeviceState");
        this.icImagingControl1.ImageAvailableExecutionMode                       =
TIS.Imaging.EventExecutionMode.MultiThreaded;
        this.icImagingControl1.LiveDisplayPosition = new System.Drawing.Point(0, 0);
        this.icImagingControl1.Location = new System.Drawing.Point(22, 23);
```

```
this.icImagingControl1.Margin = new System.Windows.Forms.Padding(2);
this.icImagingControl1.Name = "icImagingControl1";
this.icImagingControl1.Size = new System.Drawing.Size(1168, 1102);
this.icImagingControl1.TabIndex = 0;
//
// cmdStartLive
//
this.cmdStartLive.Location = new System.Drawing.Point(1281, 826);
this.cmdStartLive.Margin = new System.Windows.Forms.Padding(2);
this.cmdStartLive.Name = "cmdStartLive";
this.cmdStartLive.Size = new System.Drawing.Size(170, 59);
this.cmdStartLive.TabIndex = 1;
this.cmdStartLive.Text = "Start Live";
this.cmdStartLive.UseVisualStyleBackColor = true;
this.cmdStartLive.Click += new System.EventHandler(this.cmdStartLive_Click);
//
// cmdStopLive
//
this.cmdStopLive.Location = new System.Drawing.Point(1281, 909);
this.cmdStopLive.Margin = new System.Windows.Forms.Padding(2);
this.cmdStopLive.Name = "cmdStopLive";
this.cmdStopLive.Size = new System.Drawing.Size(170, 62);
this.cmdStopLive.TabIndex = 2;
this.cmdStopLive.Text = "Stop Live";
this.cmdStopLive.UseVisualStyleBackColor = true;
this.cmdStopLive.Click += new System.EventHandler(this.cmdStopLive_Click);
//
// cmdSaveBitmap
//
this.cmdSaveBitmap.Location = new System.Drawing.Point(1281, 990);
this.cmdSaveBitmap.Margin = new System.Windows.Forms.Padding(2);
this.cmdSaveBitmap.Name = "cmdSaveBitmap";
this.cmdSaveBitmap.Size = new System.Drawing.Size(170, 65);
this.cmdSaveBitmap.TabIndex = 3;
this.cmdSaveBitmap.Text = "Save Bitmap";
this.cmdSaveBitmap.UseVisualStyleBackColor = true;
this.cmdSaveBitmap.Click += new System.EventHandler(this.cmdSaveBitmap_Click);
//
// comboBox1
//
```

```
        this.comboBox1.FormattingEnabled = true;
        this.comboBox1.Location = new System.Drawing.Point(1321, 88);
        this.comboBox1.Margin = new System.Windows.Forms.Padding(2);
        this.comboBox1.Name = "comboBox1";
        this.comboBox1.Size = new System.Drawing.Size(115, 28);
        this.comboBox1.TabIndex = 4;
        this.comboBox1.SelectedIndexChanged += new
System.EventHandler(this.comboBox1_SelectedIndexChanged_1);
        //
        // button1
        //
        this.button1.Location = new System.Drawing.Point(1321, 131);
        this.button1.Margin = new System.Windows.Forms.Padding(2);
        this.button1.Name = "button1";
        this.button1.Size = new System.Drawing.Size(115, 62);
        this.button1.TabIndex = 5;
        this.button1.Text = "Connect";
        this.button1.UseVisualStyleBackColor = true;
        this.button1.Click += new System.EventHandler(this.button1_Click);
        //
        // button2
        //
        this.button2.Location = new System.Drawing.Point(1321, 209);
        this.button2.Margin = new System.Windows.Forms.Padding(2);
        this.button2.Name = "button2";
        this.button2.Size = new System.Drawing.Size(115, 65);
        this.button2.TabIndex = 6;
        this.button2.Text = "Setup";
        this.button2.UseVisualStyleBackColor = true;
        this.button2.Click += new System.EventHandler(this.button2_Click);
        //
        // button3
        //
        this.button3.Location = new System.Drawing.Point(1465, 439);
        this.button3.Margin = new System.Windows.Forms.Padding(2);
        this.button3.Name = "button3";
        this.button3.Size = new System.Drawing.Size(170, 65);
        this.button3.TabIndex = 7;
        this.button3.Text = "Forward";
        this.button3.UseVisualStyleBackColor = true;
```

```
this.button3.Click += new System.EventHandler(this.button3_Click);
//
// button4
//
this.button4.Location = new System.Drawing.Point(1465, 533);
this.button4.Margin = new System.Windows.Forms.Padding(2);
this.button4.Name = "button4";
this.button4.Size = new System.Drawing.Size(170, 65);
this.button4.TabIndex = 8;
this.button4.Text = "Backward";
this.button4.UseVisualStyleBackColor = true;
this.button4.Click += new System.EventHandler(this.button4_Click);
//
// textBox1
//
this.textBox1.Location = new System.Drawing.Point(1465, 619);
this.textBox1.Margin = new System.Windows.Forms.Padding(2);
this.textBox1.Name = "textBox1";
this.textBox1.Size = new System.Drawing.Size(170, 26);
this.textBox1.TabIndex = 9;
//
// button5
//
this.button5.Location = new System.Drawing.Point(1642, 109);
this.button5.Margin = new System.Windows.Forms.Padding(2);
this.button5.Name = "button5";
this.button5.Size = new System.Drawing.Size(170, 65);
this.button5.TabIndex = 10;
this.button5.Text = "ON";
this.button5.UseVisualStyleBackColor = true;
this.button5.Click += new System.EventHandler(this.button5_Click);
//
// button6
//
this.button6.Location = new System.Drawing.Point(1642, 197);
this.button6.Margin = new System.Windows.Forms.Padding(2);
this.button6.Name = "button6";
this.button6.Size = new System.Drawing.Size(170, 65);
this.button6.TabIndex = 11;
this.button6.Text = "OFF";
```

```
        this.button6.UseVisualStyleBackColor = true;
        this.button6.Click += new System.EventHandler(this.button6_Click);
        //
        // textBox2
        //
        this.textBox2.Location = new System.Drawing.Point(1642, 909);
        this.textBox2.Name = "textBox2";
        this.textBox2.Size = new System.Drawing.Size(196, 26);
        this.textBox2.TabIndex = 12;
        //
        // button7
        //
        this.button7.Location = new System.Drawing.Point(1642, 963);
        this.button7.Name = "button7";
        this.button7.Size = new System.Drawing.Size(196, 55);
        this.button7.TabIndex = 13;
        this.button7.Text = "Calculate FRET Ratio";
        this.button7.UseVisualStyleBackColor = true;
        this.button7.Click += new System.EventHandler(this.button7_Click);
        //
        // button8
        //
        this.button8.Location = new System.Drawing.Point(1642, 837);
        this.button8.Name = "button8";
        this.button8.Size = new System.Drawing.Size(196, 48);
        this.button8.TabIndex = 14;
        this.button8.Text = "Time Lapse";
        this.button8.UseVisualStyleBackColor = true;
        this.button8.Click += new System.EventHandler(this.button8_Click);
        //
        // textBox3
        //
        this.textBox3.Font = new System.Drawing.Font("Microsoft Sans Serif", 14F,
System.Drawing.FontStyle.Regular, System.Drawing.GraphicsUnit.Point, ((byte)(0)));
        this.textBox3.Location = new System.Drawing.Point(1272, 39);
        this.textBox3.Name = "textBox3";
        this.textBox3.Size = new System.Drawing.Size(216, 39);
        this.textBox3.TabIndex = 15;
        this.textBox3.Text = "Filter Swap Start";
        this.textBox3.TextChanged += new System.EventHandler(this.textBox3_TextChanged);
```

```
        //
        // textBox4
        //
        this.textBox4.Font = new System.Drawing.Font("Microsoft Sans Serif", 14F,
System.Drawing.FontStyle.Regular, System.Drawing.GraphicsUnit.Point, ((byte)(0)));
        this.textBox4.Location = new System.Drawing.Point(1590, 39);
        this.textBox4.Name = "textBox4";
        this.textBox4.Size = new System.Drawing.Size(271, 39);
        this.textBox4.TabIndex = 16;
        this.textBox4.Text = "Light Source Control";
        //
        // textBox5
        //
        this.textBox5.Font = new System.Drawing.Font("Microsoft Sans Serif", 14F,
System.Drawing.FontStyle.Regular, System.Drawing.GraphicsUnit.Point, ((byte)(0)));
        this.textBox5.Location = new System.Drawing.Point(1419, 377);
        this.textBox5.Name = "textBox5";
        this.textBox5.Size = new System.Drawing.Size(252, 39);
        this.textBox5.TabIndex = 17;
        this.textBox5.Text = "Filter Swap Control";
        this.textBox5.TextChanged += new System.EventHandler(this.textBox5_TextChanged);
        //
        // textBox6
        //
        this.textBox6.Font = new System.Drawing.Font("Microsoft Sans Serif", 14F,
System.Drawing.FontStyle.Regular, System.Drawing.GraphicsUnit.Point, ((byte)(0)));
        this.textBox6.Location = new System.Drawing.Point(1256, 762);
        this.textBox6.Name = "textBox6";
        this.textBox6.Size = new System.Drawing.Size(210, 39);
        this.textBox6.TabIndex = 18;
        this.textBox6.Text = "Camera Control";
        //
        // textBox7
        //
        this.textBox7.Font = new System.Drawing.Font("Microsoft Sans Serif", 14F,
System.Drawing.FontStyle.Regular, System.Drawing.GraphicsUnit.Point, ((byte)(0)));
        this.textBox7.Location = new System.Drawing.Point(1627, 762);
        this.textBox7.Name = "textBox7";
        this.textBox7.Size = new System.Drawing.Size(234, 39);
        this.textBox7.TabIndex = 19;
```

```
    this.textBox7.Text = "Image Processing";
    //
    // Form1
    //
    this.AutoScaleDimensions = new System.Drawing.SizeF(9F, 20F);
    this.AutoScaleMode = System.Windows.Forms.AutoScaleMode.Font;
    this.ClientSize = new System.Drawing.Size(1901, 1167);
    this.Controls.Add(this.textBox7);
    this.Controls.Add(this.textBox6);
    this.Controls.Add(this.textBox5);
    this.Controls.Add(this.textBox4);
    this.Controls.Add(this.textBox3);
    this.Controls.Add(this.button8);
    this.Controls.Add(this.button7);
    this.Controls.Add(this.textBox2);
    this.Controls.Add(this.button6);
    this.Controls.Add(this.button5);
    this.Controls.Add(this.textBox1);
    this.Controls.Add(this.button4);
    this.Controls.Add(this.button3);
    this.Controls.Add(this.button2);
    this.Controls.Add(this.button1);
    this.Controls.Add(this.comboBox1);
    this.Controls.Add(this.cmdSaveBitmap);
    this.Controls.Add(this.cmdStopLive);
    this.Controls.Add(this.cmdStartLive);
    this.Controls.Add(this.icImagingControl1);
    this.Margin = new System.Windows.Forms.Padding(2);
    this.Name = "Form1";
    this.Text = " ";
    this.Load += new System.EventHandler(this.Form1_Load_1);
    ((System.ComponentModel.ISupportInitialize)(this.icImagingControl1)).EndInit();
    this.ResumeLayout(false);
    this.PerformLayout();

}

#endregion

private TIS.Imaging.ICImagingControl icImagingControl1;
```

```
        private System.Windows.Forms.Button cmdStartLive;
        private System.Windows.Forms.Button cmdStopLive;
        private System.Windows.Forms.Button cmdSaveBitmap;
        private ComboBox comboBox1;
        private Button button1;
        private Button button2;
        private Button button3;
        private Button button4;
        private TextBox textBox1;
        private Button button5;
        private Button button6;
        private SerialPort port;
        private TextBox textBox2;
        private Button button7;
        private Button button8;
        private TextBox textBox3;
        private TextBox textBox4;
        private TextBox textBox5;
        private TextBox textBox6;
        private TextBox textBox7;
    }
}
```

Appendix L.

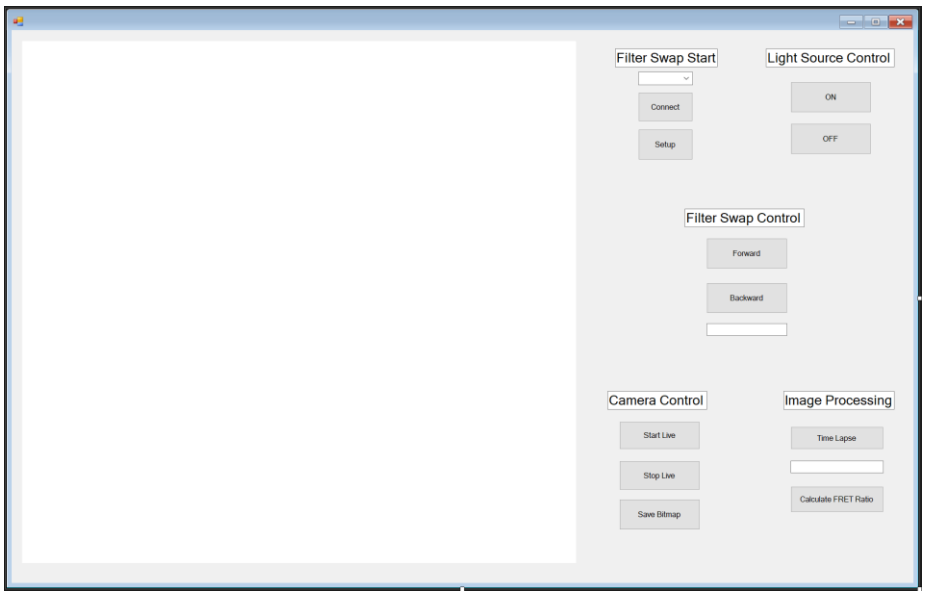
Filter Swap Start
Connect
Setup
Light Source Control
ON
OFF
Filter Swap Control
Forward
Backward
Camera Control
Start Live
Stop Live
Save Bitmap
Image Processing
Time Lapse
Calculate FRET Ratio